EUROPEAN ORGANIZATION FOR NUCLEAR RESEARCH (CERN)

CERN-EP-2018-304
2022/03/17

CMS-HIG-17-028

Measurement and interpretation of differential cross sections for Higgs boson production at $\sqrt{s} = 13\,\text{TeV}$

The CMS Collaboration*

arXiv:1812.06504v2 [hep-ex] 16 Apr 2019

Abstract

Differential Higgs boson (H) production cross sections are sensitive probes for physics beyond the standard model. New physics may contribute in the gluon-gluon fusion loop, the dominant Higgs boson production mechanism at the LHC, and manifest itself through deviations from the distributions predicted by the standard model. Combined spectra for the $\text{H} \to \gamma\gamma$, $\text{H} \to \text{ZZ}$, and $\text{H} \to \text{b}\bar{\text{b}}$ decay channels and the inclusive Higgs boson production cross section are presented, based on proton-proton collision data recorded with the CMS detector at $\sqrt{s} = 13\,\text{TeV}$ corresponding to an integrated luminosity of $35.9\,\text{fb}^{-1}$. The transverse momentum spectrum is used to place limits on the Higgs boson couplings to the top, bottom, and charm quarks, as well as its direct coupling to the gluon field. No significant deviations from the standard model are observed in any differential distribution. The measured total cross section is $61.1 \pm 6.0\,(\text{stat}) \pm 3.7\,(\text{syst})\,\text{pb}$, and the precision of the measurement of the differential cross section of the Higgs boson transverse momentum is improved by about 15% with respect to the $\text{H} \to \gamma\gamma$ channel alone.

Published in Physics Letters B as doi:10.1016/j.physletb.2019.03.059.

© 2022 CERN for the benefit of the CMS Collaboration. CC-BY-4.0 license

*See Appendix C for the list of collaboration members

1 Introduction

The Higgs boson (H), whose existence is predicted by the Brout–Englert–Higgs mechanism [1–3], is responsible for electroweak symmetry breaking in the standard model (SM). Since the discovery [4–6] of a particle compatible with the SM Higgs boson at the CERN LHC, extensive effort has been dedicated to the measurement of its properties and couplings.

In this analysis we measure the inclusive and differential cross sections for the production of Higgs bosons. Compared with inclusive measurements [7–9], differential distributions provide extended information on the Higgs boson couplings, which can be extracted by fitting parametrized spectra to a combination of differential cross sections. When the Higgs boson couplings to quarks and to other bosons are varied with respect to their SM values, distortions of the predicted differential cross section spectra appear, which are particularly pronounced in the transverse momentum (p_{T}) distribution.

A precise measurement of the Higgs boson couplings represents an important test of the SM, as the couplings are sensitive to several SM extensions [10, 11]. While the couplings to the top (y_{t}) and bottom (y_{b}) quarks are known with fair precision, there is still a relatively large uncertainty in the measurement of the couplings to lighter quarks such as the coupling to the charm quark (y_{c}). A proof-of-concept study determining limits on the modification of the SM Higgs boson coupling ($y_{\mathrm{c}}^{\mathrm{SM}}$) to the charm quark, $\kappa_{\mathrm{c}} = y_{\mathrm{c}}/y_{\mathrm{c}}^{\mathrm{SM}}$, from the Higgs boson transverse momentum ($p_{\mathrm{T}}^{\mathrm{H}}$) distribution was performed in Ref. [12]. Reinterpreting the ATLAS Collaboration measurements in Ref. [13], this analysis yields the overall bounds $\kappa_{\mathrm{c}} \in [-16, 18]$ at 95% confidence level (CL). Using the same data set, a reinterpretation of a search by the ATLAS Collaboration for the $\mathrm{H} \to \mathrm{J}/\psi\gamma$ channel [14] yields $|\kappa_{\mathrm{c}}| < 429$ at 95% CL [15]. More recently, studies from the ATLAS Collaboration [16, 17], using data collected at $\sqrt{s} = 13\,\mathrm{TeV}$ corresponding to an integrated luminosity of $36.1\,\mathrm{fb}^{-1}$, yield an observed upper limit on the $\mathrm{H} \to \mathrm{J}/\psi$ branching fraction of 3.5×10^{-4} at 95% CL that is an improvement of about a factor two with respect to the result obtained in Ref. [14], and an observed upper limit on the product of the production cross section and branching fraction $\sigma(\mathrm{pp} \to \mathrm{ZH})\mathcal{B}(\mathrm{H} \to \mathrm{c\bar{c}})$ of 110 times the SM value at 95% CL.

Both the ATLAS and CMS Collaborations have reported measurements of differential Higgs boson production cross sections at $\sqrt{s} = 8$ and 13 TeV [18–28]. The CMS Collaboration has measured differential Higgs boson production cross sections in the $\mathrm{H} \to \gamma\gamma$ [25] and $\mathrm{H} \to \mathrm{ZZ}^{(*)} \to 4\ell$ (ℓ = e or μ) [27] decay channels using data recorded by the CMS experiment in 2016 at $\sqrt{s} = 13\,\mathrm{TeV}$, corresponding to an integrated luminosity of $35.9\,\mathrm{fb}^{-1}$. We report measurements of differential cross sections obtained by combining these results. Additionally, we include a search for the Higgs boson produced with large p_{T} and decaying to a bottom quark-antiquark ($\mathrm{b\bar{b}}$) pair [29] in the combination of the $p_{\mathrm{T}}^{\mathrm{H}}$ spectra. The differential cross sections for the following observables are combined: $p_{\mathrm{T}}^{\mathrm{H}}$, the Higgs boson rapidity $|y_{\mathrm{H}}|$, the number of hadronic jets N_{jets}, and the transverse momentum of the leading hadronic jet $p_{\mathrm{T}}^{\mathrm{jet}}$.

We interpret the $p_{\mathrm{T}}^{\mathrm{H}}$ spectrum in terms of Higgs boson couplings. In order to take into account as many degrees of freedom as possible, multiple couplings are varied simultaneously. We present results obtained by varying simultaneously (i) the modifier of the Higgs boson coupling to the charm quark κ_{c} and the bottom quark κ_{b}, (ii) the modifier of the Higgs boson coupling to the top quark κ_{t} and the coefficient c_{g} of the anomalous direct coupling to the gluon field in the heavy top quark mass limit, and (iii) κ_{t} and κ_{b}.

The SM production cross sections and decay rates depend on the Higgs boson mass m_{H}. We assume a Higgs boson mass of 125.09 GeV for all measurements in this paper, based on the

combined ATLAS and CMS measurement using proton-proton collision data collected in 2011 and 2012 [8].

2 Theoretical predictions

Differential cross sections may be used to constrain model parameters. In the case of Higgs boson production via gluon fusion, the dominant production mode at the LHC, finite quark mass effects and moderate variations to Higgs boson couplings may manifest themselves through distortions of the $p_{\mathrm{T}}^{\mathrm{H}}$ spectrum. We interpret the $p_{\mathrm{T}}^{\mathrm{H}}$ spectrum for gluon fusion in terms of modifications of the couplings of the Higgs boson using two models: one tailored to heavy quarks and thus sensitive to effects at high p_{T} [30, 31], and the other considering the effect of lighter quarks in the gluon fusion loop [12]. The cross section for Higgs boson production in association with top quarks is taken to scale quadratically with κ_{t}. The other production processes are taken to be independent of these couplings. The coupling modifiers are described in the context of the κ-framework [32]:

$$\kappa_i = \frac{y_i}{y_i^{\mathrm{SM}}}, \tag{1}$$

where y_i is the Higgs boson coupling to particle i. The SM value of any κ_i is equal to 1.

Recent developments in p_{T} resummation procedures have allowed more accurate calculations of the $p_{\mathrm{T}}^{\mathrm{H}}$ spectrum when including the effects of lighter quarks on Higgs boson production via gluon fusion [33–36]. The $p_{\mathrm{T}}^{\mathrm{H}}$ spectrum for gluon fusion has been calculated for simultaneous variations of κ_{c} and κ_{b} [12], taking into account the interference of the top quark loop with that from the bottom and charm quarks in the gluon fusion production loop, providing a novel approach to constrain these couplings via the $p_{\mathrm{T}}^{\mathrm{H}}$ spectrum. We parameterize the variations computed in Ref. [12] with a quadratic polynomial for each bin of the $p_{\mathrm{T}}^{\mathrm{H}}$ spectrum. The Higgs boson coupling to the top quark is fixed to its SM value in this model. The calculations from Ref. [12] are given up to the scale of the Higgs boson mass, and thus the $\mathrm{H} \to \mathrm{b\bar{b}}$ channel (for which the lower limit of the $p_{\mathrm{T}}^{\mathrm{H}}$ spectrum is 350 GeV) is not used as input for the results obtained with this model.

A second model producing simultaneous variations of κ_{t}, c_{g}, and κ_{b} by adding dimension-6 operators to the SM Lagrangian has been built in Refs. [30, 31]. This study employs an analytic resummation performed up to next-to-next-to-leading-logarithmic (NNLL) order in order to obtain the $p_{\mathrm{T}}^{\mathrm{H}}$ spectrum at next-to-next-to-leading order+NNLL (NNLO+NNLL) accuracy. The dimension-6 operator whose coefficient is c_{g} yields a direct coupling of the Higgs field to the gluon field with the same underlying tensor structure as in the heavy-top mass limit. In the SM, the value of c_{g} equals 0. The introduction of c_{g} in the effective Lagrangian is given in Ref. [31] and the inclusive cross section is given by $\sigma \simeq \left|12c_{\mathrm{g}} + \kappa_{\mathrm{t}}\right|^2 \sigma^{\mathrm{SM}}$. Two other operators are included in the Lagrangian to describe modifications of the top and bottom Yukawa couplings with coefficients κ_{t} and κ_{b}, respectively. While the model allows simultaneous variation of all three coupling modifiers, we consider only simultaneous variations of κ_{t} and c_{g}, and of κ_{t} and κ_{b}. The precomputed spectra from Ref. [30] are used as input and parametrized using a quadratic polynomial.

3 The CMS detector

The central feature of the CMS apparatus is a superconducting solenoid of 6 m internal diameter, providing a magnetic field of 3.8 T. Within the solenoid volume are a silicon pixel and strip

tracker, a lead tungstate crystal electromagnetic calorimeter, and a brass and scintillator hadron calorimeter, each composed of a barrel and two endcap sections. Forward calorimeters extend the pseudorapidity (η) coverage provided by the barrel and endcap detectors. Muons are detected in gas-ionization chambers embedded in the steel flux-return yoke outside the solenoid. A more detailed description of the CMS detector, together with a definition of the coordinate system used and the relevant kinematic variables, can be found in Ref. [37].

4 Inputs to the combined analysis

For all the analyses used as input to the combination ($\mathrm{H} \to \gamma\gamma$ [25], $\mathrm{H} \to \mathrm{ZZ}^{(*)} \to 4\ell$ [27], and $\mathrm{H} \to \mathrm{b\bar{b}}$ [29]), the data set corresponds to an integrated luminosity of 35.9 fb^{-1} recorded by the CMS experiment in 2016. The $\mathrm{H} \to \mathrm{b\bar{b}}$ decay channel is only included in the combination of the $p_{\mathrm{T}}^{\mathrm{H}}$ spectra, improving the measurements at the higher end of the distribution where the data from the $\mathrm{H} \to \gamma\gamma$ and $\mathrm{H} \to \mathrm{ZZ}$ decay channels are limited. All analyses provide the parametrization of the folding matrix M_{ji}^{k} (which is the probability for an event in generator-level bin i to be reconstructed in bin j and category k) in terms of a common generator-level binning, that is used for the combined spectra. Given the limited statistical precision in the individual channels, the results of the $\mathrm{H} \to \mathrm{ZZ}$ and $\mathrm{H} \to \mathrm{b\bar{b}}$ channels individually are reported for a coarser binning, which is provided in Tables 1–4 for each of the observables. This binning coincides with the binning at the reconstruction level.

The SM prediction for the differential cross sections is simulated with MADGRAPH5_*a*MC@NLO v2.2.2 [38] for each of the four dominant Higgs boson production modes: gluon-gluon fusion (ggH), vector boson fusion, associated production with a W/Z boson, and associated production with a top quark-antiquark pair. A contribution from Higgs boson production in association with bottom quarks is not simulated, but included assuming its acceptance is equal to that from Higgs boson production via gluon fusion. The matrix element calculation includes the emission of up to two additional partons and is performed at NLO accuracy in perturbative quantum chromodynamics (QCD). Events are interfaced to PYTHIA 8.205 [39] for parton showering and hadronization with the CUETP8M1 [40] underlying event tune. The matrix element calculation is matched to the parton shower following the prescription in Ref. [41]. A weight depending on $p_{\mathrm{T}}^{\mathrm{H}}$ and N_{jets} is applied to simulated ggH events to match the predictions from the NNLOPS program [42, 43], as discussed in Ref. [9]. The set of parton distribution functions used in all simulations is NNPDF3.0 [44]. The hadronic jets are clustered from the particle-flow candidates [45] in the case of data and simulation, and from stable particles excluding neutrinos in the case of generated events, using the anti-k_{T} clustering algorithm [46] with a distance parameter of 0.4. The measurements are reported in terms of kinematic observables defined before the decay of the Higgs boson, i.e. at the generator level.

Each of the analyses used as input to the combination corresponds to a different fiducial phase space definition and applies a different event categorization. In the case of the $\mathrm{H} \to \gamma\gamma$ analysis, the fiducial phase space is defined by requiring the ratio of the leading (subleading) photon p_{T} to the diphoton mass to be greater than 1/3 (1/4). In addition, for each photon candidate the scalar sum of the generator-level p_{T} of stable particles contained in a cone of radius $\Delta R = 0.3$ around the candidate is required to be less than 10 GeV, where $\Delta R = \sqrt{(\Delta\eta)^2 + (\Delta\phi)^2}$ is the angular separation between particles and $\Delta\phi$ is the azimuthal angle between two particles in radians. The selected photon pairs are categorized according to their estimated relative invariant mass resolution [25]. In the case of the $\mathrm{H} \to \mathrm{ZZ}$ analysis, the 4-lepton mass is required to be greater than 70 GeV, the leading Z boson candidate invariant mass must be greater than 40 GeV, and leptons must be separated in angular space by at least $\Delta R > 0.02$. Furthermore, at

least two leptons must each have a $p_T > 10\,\text{GeV}$ and at least one a $p_T > 20\,\text{GeV}$. The selected events are categorized according to their lepton configuration in the final state (4 electrons, 4 muons, or 2 electrons and 2 muons). In the case of the $H \to b\bar{b}$ analysis, the analysis strategy requires the presence of a single anti-k_T jet with a distance parameter of 0.8, $p_T > 450\,\text{GeV}$, and $|\eta| < 2.5$. For this analysis, the data is not unfolded to a fiducial phase space. Soft and wide-angle radiation is removed using the soft-drop grooming algorithm [47, 48]. The jet mass after application of the soft-drop algorithm, m_{SD}, peaks close to the Higgs boson mass in the case of signal events. To avoid finite-cone effects and the nonperturbative regime of the m_{SD} calculation, events are selected based on the dimensionless mass scale variable for QCD jets defined as $\rho = \log\left(m_{SD}^2/p_T^2\right)$ [47], which relates the jet p_T to the jet mass. Events with isolated electrons, muons, or τ leptons with $p_T > 10\,\text{GeV}$ and $|\eta| < 2.5$ are vetoed in order to reduce the background from SM electroweak processes, and events with a missing transverse momentum greater than 140 GeV are vetoed in order to reduce the background from top quark-antiquark pair production. Additionally, a selection criterion is applied based on the compatibility of the single anti-k_T jet with having a two-prong substructure [49–52]. Events are categorized according to their likelihood of consisting of two b quarks, which is computed using the double-b tagger algorithm [53].

Minor modifications are applied to the individual analyses in Refs. [25, 27, 29] to provide the inputs used for the combination of differential observables. For $H \to \gamma\gamma$, an additional bin, $p_T^H > 600\,\text{GeV}$, is included in the p_T^H spectrum. For $H \to ZZ$, the binning is modified for multiple kinematic observables to align with the binning of the $H \to \gamma\gamma$ analysis. Furthermore, the branching fractions of the two Z bosons to the various lepton configurations are fixed to their SM values, whereas in Ref. [27] these are allowed to float. For $H \to b\bar{b}$ the signal is split into two p_T bins at the generator level: the first with $350 \leq p_T < 600\,\text{GeV}$, where the lower limit has been extended downwards with respect to the individual analysis, and the second an overflow bin with $p_T \geq 600\,\text{GeV}$, which aligns with the binning of the other channels. At the reconstruction level two bins are employed, with $450 \leq p_T < 600$ and $p_T \geq 600\,\text{GeV}$, which is a slight modification with respect to the binning used in Ref. [29]. The redefinition of the reconstructed p_T categories necessitates a reevaluation of the background model, which is performed using the same procedure as in the original analysis. For the purpose of the combination in this analysis, the fiducial measurements from the $H \to \gamma\gamma$ and $H \to ZZ$ channels are extrapolated to the inclusive phase space [38, 42, 43].

Table 1: The reconstruction-level binning for p_T^H for the $H \to \gamma\gamma$, $H \to ZZ$, and $H \to b\bar{b}$ channels. This binning coincides with the binning of the unfolded cross sections in which the individual results are reported.

Channel	p_T^H binning (GeV)								
$H \to \gamma\gamma$	[0, 15)	[15, 30)	[30, 45)	[45, 80)	[80, 120)	[120, 200)	[200, 350)	[350, 600)	[600, ∞)
$H \to ZZ$	[0, 15)	[15, 30)	[30, 80)		[80, 200)		[200, ∞)		
$H \to b\bar{b}$	None							[350, 600)	[600, ∞)

Table 2: The binning for N_{jets} for the $H \to \gamma\gamma$ and the $H \to ZZ$ channels. This binning coincides with the binning of the unfolded cross sections in which the individual results are reported.

Channel	N_{jets} binning				
$H \to \gamma\gamma$	0	1	2	3	≥ 4
$H \to ZZ$	0	1	2	≥ 3	

Table 3: The binning for $|y_{\mathrm{H}}|$ for the $\mathrm{H} \to \gamma\gamma$ and the $\mathrm{H} \to \mathrm{ZZ}$ channels. This binning coincides with the binning of the unfolded cross sections in which the individual results are reported.

Channel	$\lvert y_{\mathrm{H}} \rvert$ binning					
$\mathrm{H} \to \gamma\gamma$	[0.0, 0.15)	[0.15, 0.30)	[0.30, 0.60)	[0.60, 0.90)	[0.90, 1.20)	[1.20, 2.50]
$\mathrm{H} \to \mathrm{ZZ}$	[0.0, 0.15)	[0.15, 0.30)	[0.30, 0.60)	[0.60, 0.90)	[0.90, 1.20)	[1.20, 2.50]

Table 4: The binning for $p_{\mathrm{T}}^{\mathrm{jet}}$ for the $\mathrm{H} \to \gamma\gamma$ and the $\mathrm{H} \to \mathrm{ZZ}$ channels. This binning coincides with the binning of the unfolded cross sections in which the individual results are reported.

Channel	$p_{\mathrm{T}}^{\mathrm{jet}}$ binning (GeV)					
$\mathrm{H} \to \gamma\gamma$	[0, 30)	[30, 55)	[55, 95)	[95, 120)	[120, 200)	[200, ∞)
$\mathrm{H} \to \mathrm{ZZ}$	[0, 30)	[30, 55)	[55, 95)	[95, ∞)		

5 Statistical analysis

The cross sections are extracted through a simultaneous extended maximum likelihood fit to the diphoton mass, four-lepton mass, and m_{SD} distributions in all the analysis categories of the $\mathrm{H} \to \gamma\gamma$, $\mathrm{H} \to \mathrm{ZZ}$, and $\mathrm{H} \to \mathrm{b\overline{b}}$ channels, respectively.

The number of expected signal events n^{sig} in a given reconstructed kinematic bin i, given analysis category k and given decay channel m is obtained from:

$$n_i^{\mathrm{sig},\,km}(\vec{\Delta\sigma}|\vec{\theta}) = \sum_{j=1}^{n_{\mathrm{bins}}^{\mathrm{gen}}} \Delta\sigma_j \, L(\vec{\theta}) \, \mathcal{B}^m \, M_{ji}^{km}(\vec{\theta}), \tag{2}$$

where:

- j is a kinematic bin index at the generator level;
- $n_{\mathrm{bins}}^{\mathrm{gen}}$ is the number of kinematic bins at the generator level, which is the same for all decay channels;
- $\vec{\Delta\sigma}$ is the set of differential cross sections at the generator level, and L is the integrated luminosity of the samples used in this analysis;
- $\mathcal{B}^m$ is the branching fraction of the decay channel m. The overall effect of the branching fraction uncertainties on the combined spectra is below 1%, and has been neglected.
- M_{ji}^{km} is the folding matrix, which is determined from Monte Carlo simulation; note that the corresponding matrix $\vec{M}^{\,km}$ need not be square; the number of reconstructed bins may be smaller than the number of bins at the generator level; and
- $\vec{\theta}$ is the set of nuisance parameters.

The bin-to-bin migrations are taken into account via the folding matrix, effectively allowing unfolding of the detector effects. Following the prescription in Ref. [54], we find that no regularization of the unfolding procedure is needed.

An extended likelihood function for a single decay channel m is constructed:

$$\mathcal{L}_m(\vec{\Delta\sigma}|\vec{\theta}) = \prod_{i=1}^{n_{\mathrm{bins}}^{\mathrm{reco},\,m}} \prod_{k=1}^{n_{\mathrm{cat}}^{m}} \prod_{l=1}^{n_{\mathcal{O}}^{m}} \left(\mathrm{pdf}_i^{km}(\mathcal{O}_l^m|\vec{\Delta\sigma},\vec{\theta}) \right)^{N_{\mathrm{obs}}^{iklm}} \times \mathrm{Poisson}\left(N_{\mathrm{obs}}^{ikm} \,\middle|\, n_i^{\mathrm{sig},\,km}(\vec{\Delta\sigma}|\vec{\theta}) + n_i^{\mathrm{bkg},\,km}(\vec{\theta}) \right), \tag{3}$$

where:

- $\mathcal{O}^m$ is the observable, i.e. the diphoton mass, the four-lepton mass, or m_{SD} for the $\mathrm{H} \to \gamma\gamma$, $\mathrm{H} \to \mathrm{ZZ}$, and $\mathrm{H} \to \mathrm{b\bar{b}}$ decay channels, respectively;
- $n_{\mathrm{bins}}^{\mathrm{reco},m}$ is the number of reconstructed bins, n_{cat}^m is the number of categories for the decay channel (see the individual analyses [25, 27, 29] for more details), and $n_{\mathcal{O}}^m$ is the number of bins for observable $\mathcal{O}$;
- N_{obs}^{iklm} is the number of observed events reconstructed in kinematic bin i, category k and observable bin l, and N_{obs}^{ikm} is the same but summed over all bins of the observable;
- $n_i^{\mathrm{bkg},km}$ is the number of expected background events; and
- $\mathrm{pdf}_i^{km}(\mathcal{O}_l^m|\vec{\Delta\sigma},\vec{\theta})$ is the probability density function for the observable, based on the signal and background distributions of the observable which are determined via simulation.

In order to combine the decay channels, the likelihoods for the individual decay channels are multiplied:

$$\mathcal{L}(\vec{\Delta\sigma}|\vec{\theta}) = \prod_{m=1}^{n_c} \mathcal{L}_m(\vec{\Delta\sigma}|\vec{\theta})\,\mathrm{pdf}(\vec{\theta}), \tag{4}$$

where n_c is the number of decay channels included in the combination, $\mathcal{L}_m$ is the likelihood formula from Eq. (3) specific to the decay channel m, and $\mathrm{pdf}(\vec{\theta})$ is the probability density function of the nuisance parameters. For the individual analyses, the number of categories, invariant mass bins, and even the number of reconstructed bins may differ, although the number of bins at the generator level and their binning need to be aligned between decay channels. Note that a single common set of differential cross sections and nuisance parameters is fitted to the data in all decay channels simultaneously.

The test statistic q, which is asymptotically distributed as a χ^2, is defined as [55, 56]:

$$q(\vec{\Delta\sigma}) = -2\,\ln\left(\frac{\mathcal{L}\left(\vec{\Delta\sigma}\,\middle|\,\hat{\hat{\vec{\theta}}}_{\vec{\Delta\sigma}}\right)}{\mathcal{L}\left(\hat{\vec{\Delta\sigma}}\,\middle|\,\hat{\vec{\theta}}\right)}\right). \tag{5}$$

The quantities $\hat{\vec{\Delta\sigma}}$ and $\hat{\vec{\theta}}$ are the unconditional maximum likelihood estimates for the parameters $\vec{\Delta\sigma}$ and $\vec{\theta}$, respectively, while $\hat{\hat{\vec{\theta}}}_{\vec{\Delta\sigma}}$ denotes the maximum likelihood estimate for $\vec{\theta}$ conditional on the values of $\vec{\Delta\sigma}$.

The Higgs boson coupling modifiers are fitted via a largely analogous procedure. In the likelihood function (4), the differential cross sections $\vec{\Delta\sigma}$ are replaced by parametrizations of theoretical spectra, instead of allowing them to be determined in the fit:

$$\vec{\Delta\sigma} \;\to\; \vec{\Delta\sigma}(\kappa_{\mathrm{a}},\kappa_{\mathrm{b}}), \tag{6}$$

where κ_{a} and κ_{b} are the coupling modifiers to be fitted.

6 Systematic uncertainties

The experimental systematic uncertainties from the input analyses are incorporated in the combination as nuisance parameters in the extended likelihood fit and are profiled. Among the

decay channels, correlations are taken into account for the systematic uncertainties in the jet energy scale and resolution, and the integrated luminosity. Detailed descriptions of the experimental systematic uncertainties per decay channel can be found in Refs. [25, 27, 29].

The measurement is made for the full phase space rather than limited to a fiducial phase space (as is the case for the original $H \to \gamma\gamma$ and $H \to ZZ$ analyses). This means that the uncertainties in the acceptances for the individual analyses and in the branching fractions may affect the results. The effect of the acceptance uncertainties per bin on the overall uncertainty, including the effect of the Higgs coupling modifiers on the acceptances, is less than 1% and so this is neglected in the combination. For certain measurements the production cross sections of non-ggH production modes are assumed to be their respective SM value. In these cases, the uncertainty in the inclusive production cross section from non-ggH modes, determined to be about 2.1% [57], has been taken into account as a nuisance parameter.

The theoretical predictions described in Section 2 are subject to theoretical uncertainties from the renormalisation scale μ_R and the factorisation scale μ_F. The standard approach to evaluate the impact of these uncertainties is to compute an envelope of scale variations, and to assign the extrema of the envelope as the uncertainty. To this end, μ_R and μ_F are independently varied between 0.5, 1, and 2 times their nominal value, whereas the fraction $\frac{\mu_R}{\mu_F}$ is constrained not to be less than 0.5 or greater than 2.0. As the theoretical spectra in the $\kappa_t/c_g/\kappa_b$ case and the κ_c/κ_b case contain a resummation, the uncertainty in the resummation scale Q is also considered, and it is evaluated by varying Q from 0.5 to 2 times its central value (while keeping μ_F and μ_R at their respective central values). The theoretical uncertainties are assigned by applying the minimum and maximum scale variations per bin. The resulting uncertainties for the spectra under variations of κ_b and κ_c and variations of κ_t, c_g, and κ_b are shown in Tables 5 and 6, respectively.

Table 5: Uncertainties in the predicted p_T^H spectra related to variations of theory parameters for the κ_b and κ_c case.

Binning (GeV)	[0, 15)	[15, 30)	[30, 45)	[45, 80)	[80, 120)
Δ^{scale} (%)	8.9%	6.6%	18.1%	22.0%	21.6%

Table 6: Uncertainties in the predicted p_T^H spectra related to variations of theory parameters for the κ_t, c_g, and κ_b case.

Binning (GeV)	[0, 15)	[15, 30)	[30, 45)	[45, 80)	[80, 120)	[120, 200)	[200, 350)	[350, 600)	[600, 800)
Δ^{scale} (%)	12.7%	7.4%	9.5%	12.8%	17.4%	19.3%	20.9%	23.4%	8.2%

Theoretical uncertainties are subject to bin-to-bin correlations. We adopt a procedure that produces a correlation coefficient ρ_{ab} directly from the individual scale variations:

$$\rho_{ab} = \frac{\sum_i (\sigma_{a,i} - \overline{\sigma}_a)(\sigma_{b,i} - \overline{\sigma}_b)}{\sqrt{\sum_i (\sigma_{a,i} - \overline{\sigma}_a)^2 \sum_i (\sigma_{b,i} - \overline{\sigma}_b)^2}}, \tag{7}$$

where $\sigma_{a(b),i}$ is the cross section in bin a (b) of the ith scale variation, $\overline{\sigma}_{a(b)}$ is the mean cross section in bin a (b), and ρ_{ab} is the resulting correlation coefficient between bin a and b. The correlation structure is characterized by strong correlations among bins at moderate p_T^H ($15 \leq p_T^H \leq 600\,\text{GeV}$). Only the bins with $p_T^H < 15$ and $p_T^H > 600\,\text{GeV}$ are anti-correlated with the bins at moderate p_T^H.

7 Results

7.1 Total cross section and $\mathcal{B}_{\gamma\gamma}/\mathcal{B}_{ZZ}$

The total cross section for Higgs boson production, based on a combination of the $H \to \gamma\gamma$ and $H \to ZZ$ channels, is measured to be $61.1 \pm 6.0\,(\text{stat}) \pm 3.7\,(\text{syst})$ pb, obtained by applying the treatment described in Section 4 to the inclusive cross section (i.e. with a single bin, both at generator and at reconstruction level). The measured total cross sections from the individual channels are 64.0 ± 9.6 pb for $H \to \gamma\gamma$ and 58.2 ± 9.8 pb for $H \to ZZ$; the combination improves the precision by 27% with respect to the $H \to \gamma\gamma$ channel individually. The likelihood scans for the individual decay channels and their combination are shown in Fig. 1 (left). The combination result agrees with the SM value of 55.6 ± 2.5 pb [57].

A measurement of the branching fraction for one decay channel is degenerate with a measurement of the total cross section. However, the ratio of branching fractions for two decay channels can be measured while profiling the total cross section. The ratio of the $H \to \gamma\gamma$ and $H \to ZZ$ branching fractions, $\mathcal{B}_{\gamma\gamma}/\mathcal{B}_{ZZ}$, is measured to be $0.092 \pm 0.018\,(\text{stat}) \pm 0.010\,(\text{syst})$. This is in agreement with the SM prediction of 0.086 ± 0.002 [57]. The likelihood scan for $\mathcal{B}_{\gamma\gamma}/\mathcal{B}_{ZZ}$ is shown in Fig. 1 (right).

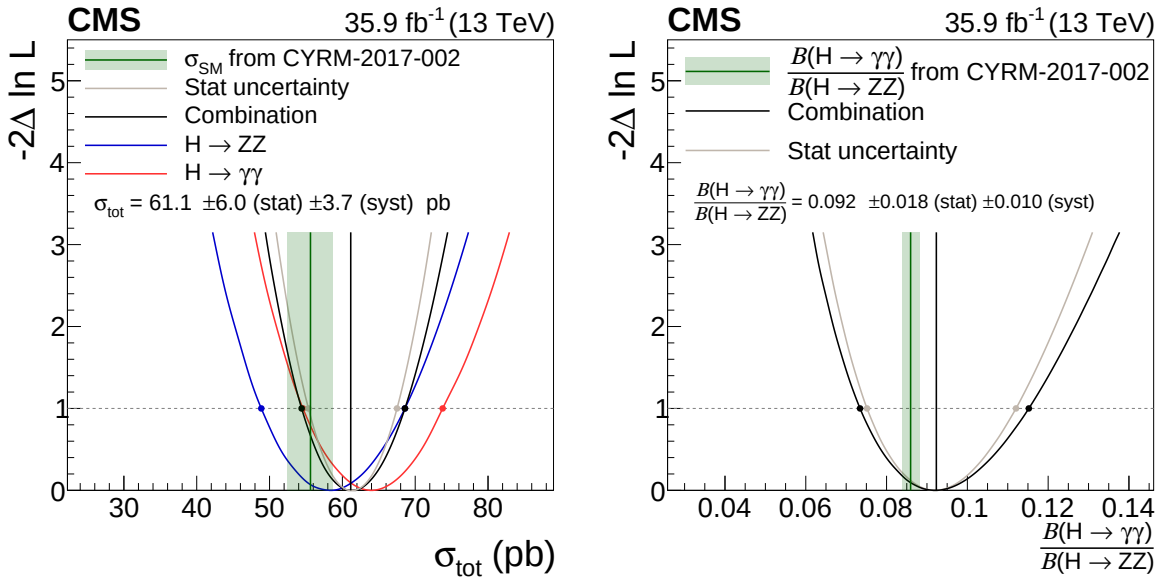

Figure 1: Scan of the total cross section σ_{tot} (left) and of the ratio of branching fractions $\mathcal{B}_{\gamma\gamma}/\mathcal{B}_{ZZ}$ (right), based on a combination of the $H \to \gamma\gamma$ and $H \to ZZ$ analyses. The markers indicate the one standard deviation confidence interval. *CYRM-2017-002* refers to Ref. [57].

7.2 Combinations of differential observables

The unfolded differential cross sections for the observables p_{T}^{H}, N_{jets}, $|y_{\text{H}}|$, and $p_{\text{T}}^{\text{jet}}$ are shown in Figs. 2, 3, 4, and 5, respectively. Figure 2 (right) shows the differential cross section of p_{T}^{H} for Higgs boson production via gluon fusion; for this result, the non-gluon-fusion production modes are considered to be background, constrained to the SM predictions with their respective uncertainties. The numerical values for the spectra in Figs. 2–5 are given in Appendix A and the corresponding bin-to-bin correlation matrices are given in Appendix B. For the observables p_{T}^{H}, N_{jets}, and $p_{\text{T}}^{\text{jet}}$, the rightmost bin is an overflow bin, which is normalized by the bin width of the second-to-rightmost bin. Overall no significant deviations from the SM predictions are

observed. For the p_T^H spectrum, the dominant source of uncertainty is the statistical one; in particular, the systematic uncertainty is about half the statistical uncertainty in the rightmost bin, and much smaller than the statistical uncertainty in all other bins. The total uncertainty in the combination per bin varies between 30 and 40%. Compared to the measurement in the $H \to \gamma\gamma$ channel alone, the decrease in uncertainty achieved by the combination is most notable in the low-p_T region. The contribution of the $H \to b\bar{b}$ channel to the overall precision of the combination is most significant in the last p_T^H bin.

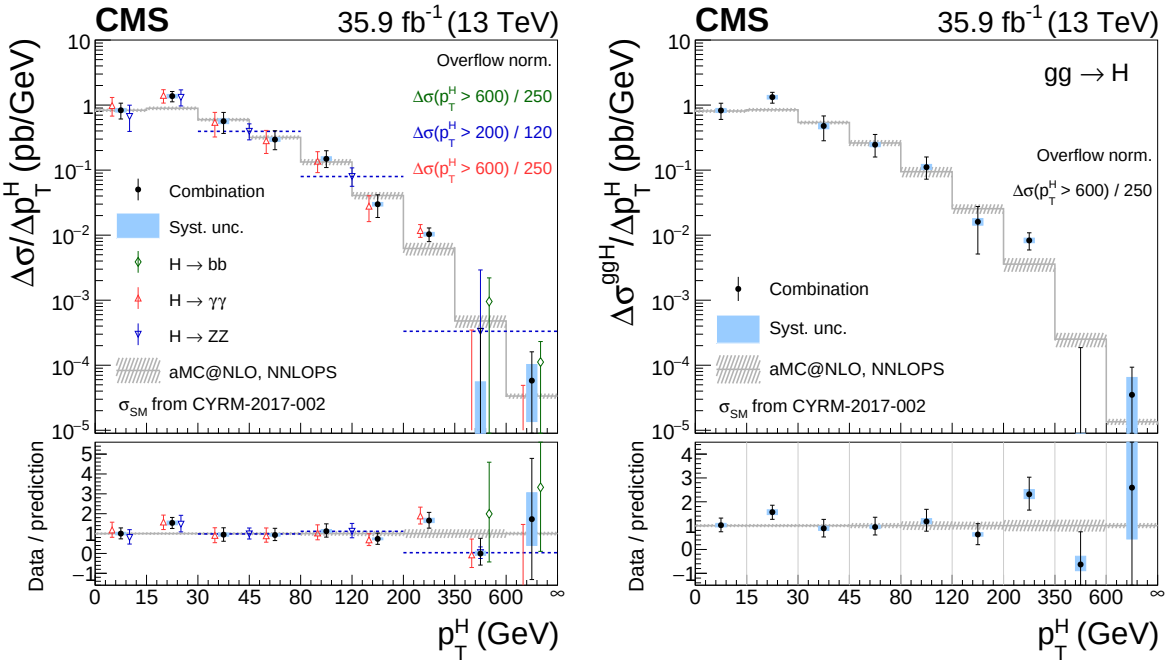

Figure 2: Measurement of the total differential cross section (left) and the differential cross section of gluon fusion (right) as a function of p_T^H. The combined spectrum is shown as black points with error bars indicating a 1 standard deviation uncertainty. The systematic component of the uncertainty is shown by a blue band. The spectra for the $H \to \gamma\gamma$, $H \to ZZ$, and $H \to b\bar{b}$ channels are shown in red, blue, and green, respectively. The dotted horizontal lines in the $H \to ZZ$ channel indicate the coarser binning of this measurement. The rightmost bins of the distributions are overflow bins; the normalizations of the cross sections in these bins are indicated in the figure. *CYRM-2017-002* refers to Ref. [57].

7.3 Fits of Higgs boson coupling modifiers: κ_b vs. κ_c

Figure 6 (left) shows the one and two standard deviation contours of the fits of the κ_b/κ_c parametrization from Ref. [12] to data, assuming the branching fractions are dependent on the Higgs boson couplings, i.e., $\mathcal{B} = \mathcal{B}(\kappa_b, \kappa_c)$, and that there are no beyond-the-SM contributions. The substructure on the combined scan shows a ring shape around the origin, in agreement with the SM prediction within one standard deviation.

In order to assess the constraint obtained only from the knowledge of the p_T^H distribution, the total width and the overall normalization are profiled in the fit. This is effectively accomplished by implementing the branching fractions for the $H \to \gamma\gamma$ and $H \to ZZ$ channels as nuisance parameters with no prior constraint, i.e. as free parameters. The result of this fit is shown in Fig. 6 (right). As expected, the range of allowed values of κ_b and κ_c is much wider than in the case of coupling-dependent branching fractions.

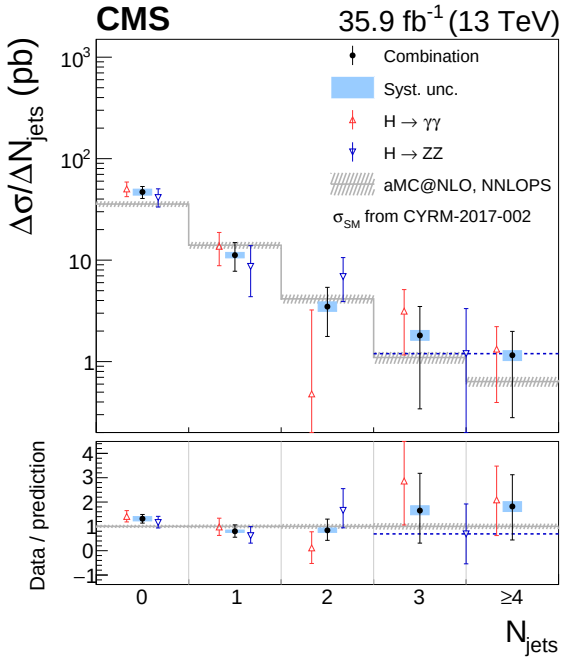

Figure 3: Measurement of the differential cross section as a function of N_{jets}. The combined spectrum is shown as black points with error bars indicating a 1 standard deviation uncertainty. The systematic component of the uncertainty is shown by a blue band. The spectra for the $\mathrm{H} \to \gamma\gamma$ and $\mathrm{H} \to \mathrm{ZZ}$ channels are shown in red and blue, respectively. The dotted horizontal lines in the $\mathrm{H} \to \mathrm{ZZ}$ channel indicate the coarser binning of this measurement. *CYRM-2017-002* refers to Ref. [57].

Confidence intervals can be set on κ_b and κ_c by profiling one coupling and scanning over the other. The results of these single-coupling scans are shown in Figs. 7 and 8. The observed (expected) limits at 95% CL in the one-dimensional scans are:

$$\begin{aligned} -1.1 < \kappa_\mathrm{b} < 1.1 \quad (-1.3 < \kappa_\mathrm{b} < 1.3), \\ -4.9 < \kappa_\mathrm{c} < 4.8 \quad (-6.1 < \kappa_\mathrm{c} < 6.0), \end{aligned} \tag{8}$$

in the case of branching fractions that depend on κ_b and κ_c, and

$$\begin{aligned} -8.5 < \kappa_\mathrm{b} < 18 \quad (-8.8 < \kappa_\mathrm{b} < 15), \\ -33 < \kappa_\mathrm{c} < 38 \quad (-31 < \kappa_\mathrm{c} < 36), \end{aligned} \tag{9}$$

in the case of the branching fractions implemented as nuisance parameters with no prior constraint. For the coupling-dependent branching fractions, the results are shaped predominantly by the constraints from the total width rather than by distortions of the p_T^H spectrum. If the branching fractions are fixed to their SM expectations, the one-dimensional scans yield the following expected limits at 95% CL:

$$\begin{aligned} -3.5 < \kappa_\mathrm{b} < 5.1, \\ -13 < \kappa_\mathrm{c} < 15. \end{aligned} \tag{10}$$

These intervals are comparable to those in Ref. [12], where $\kappa_\mathrm{c} \in [-16, 18]$ at 95% CL, noting that the results here are based on a larger data set. The intervals obtained are competitive with the intervals from other direct search channels summarized in Section 1.

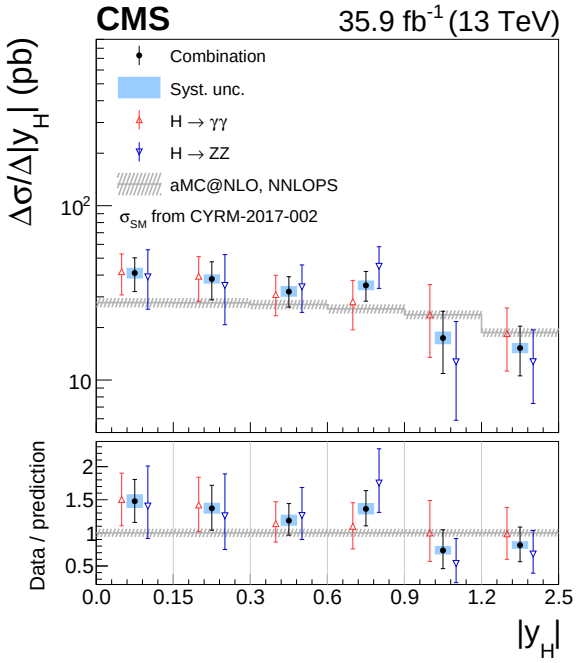

Figure 4: Measurement of the differential cross section as a function of $|y_H|$. The combined spectrum is shown as black points with error bars indicating a 1 standard deviation uncertainty. The systematic component of the uncertainty is shown by a blue band. The spectra for the $H \to \gamma\gamma$ and $H \to ZZ$ channels are shown in red and blue, respectively. *CYRM-2017-002* refers to Ref. [57].

7.4 Fits of Higgs boson coupling modifiers: κ_t vs. c_g and κ_t vs. κ_b

The fits are repeated in a way analogous to that of Section 7.3 but with κ_t, c_g, and κ_b, the coefficients of the dimension-6 operators added to the SM Lagrangian, as the parameters of the fit, using the parametrization obtained from Refs. [30, 31]. The combined log-likelihood scan for κ_t vs. c_g, assuming branching fractions that depend on the couplings, is shown in Fig. 9 (left). The normalization of the spectrum is, by construction, equal to the SM normalization for the set of coefficients satisfying $12c_g + \kappa_t \simeq 1$. The shape of the parametrized p_T^H spectrum s is calculated by normalizing the differential cross section to 1:

$$s_i(\kappa_t, c_g) = \frac{\sigma_i(\kappa_t, c_g)}{\sum_j \sigma_j(\kappa_t, c_g)}, \tag{11}$$

where σ_i is the parametrization in bin i. Inserting the expected parabolic dependence of $\sigma_i(\kappa_t, c_g)$ reveals that the shape of the parametrization for κ_t/c_g variations becomes a function of the ratio of the two couplings, $s_i(c_g/\kappa_t)$. Thus the dependence of the likelihood on the radial distance $\sqrt{\kappa_t^2 + c_g^2}$ stems from constraints on the overall normalization, whereas the dependence on the slope c_g/κ_t stems from constraints on the shape of the distribution. The dependence of the likelihood on the slope becomes apparent in Fig. 9 (right), where the branching fractions are implemented as nuisance parameters with no prior constraint in the fit. Except at small values of the couplings, the constraint on the couplings comes from their ratio. The two symmetric sets of contours are due to a symmetry of the parametrization under $(\kappa_t, c_g) \to (-\kappa_t, -c_g)$. The constraint from the $H \to \gamma\gamma$ channel individually is here slightly stronger than the combination; this effect, not observed in expected fits, stems from opposite deviations in the $H \to \gamma\gamma$ and $H \to ZZ$ p_T^H spectra that cancel out in the combination.

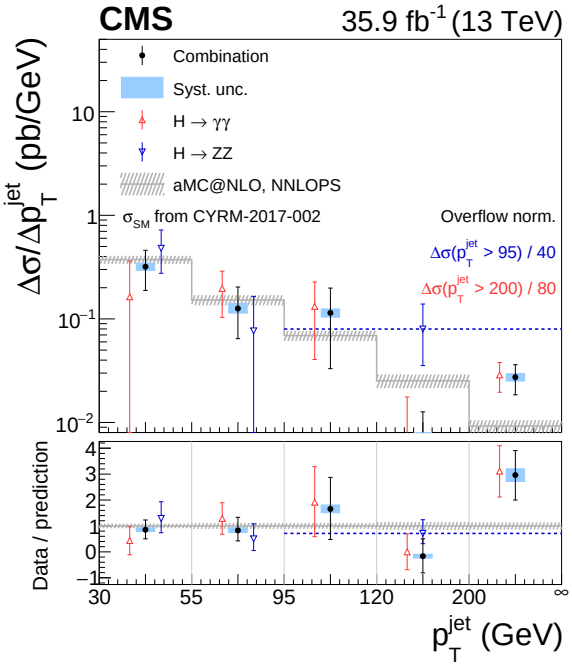

Figure 5: Measurement of the differential cross section as a function of $p_{\mathrm{T}}^{\mathrm{jet}}$. The combined spectrum is shown as black points with error bars indicating a 1 standard deviation uncertainty. The systematic component of the uncertainty is shown by a blue band. The spectra for the $\mathrm{H} \to \gamma\gamma$ and $\mathrm{H} \to \mathrm{ZZ}$ channels are shown in red and blue, respectively. The dotted horizontal lines in the $\mathrm{H} \to \mathrm{ZZ}$ channel indicate the coarser binning of this measurement. The rightmost bin of the distribution is an overflow bin; the normalization of the cross section in that bin is indicated in the figure. *CYRM-2017-002* refers to Ref. [57].

Figure 10 (left) shows the combined log-likelihood scan as a function of κ_{t} and κ_{b}, with branching fractions scaling appropriately with the coupling modifiers and Fig. 10 (right) with the branching fractions implemented as nuisance parameters with no prior constraint. As the $\mathrm{H} \to \gamma\gamma$ branching fraction depends linearly on κ_{t}, the constraints on the $\mathrm{H} \to \gamma\gamma$ channel and the combination in Fig. 10 (left) are not symmetric with respect to the κ_{t} axis. For the branching fractions implemented as nuisance parameters with no prior constraint, the parametrization is symmetric under $(\kappa_{\mathrm{t}}, \kappa_{\mathrm{b}}) \to (-\kappa_{\mathrm{t}}, -\kappa_{\mathrm{b}})$, which explains the observed symmetry in Fig. 10 (right).

8 Summary

A combination of differential cross sections for the Higgs boson transverse momentum $p_{\mathrm{T}}^{\mathrm{H}}$, the number of jets, the rapidity of the Higgs boson, and the p_{T} of the leading jet has been presented, using proton-proton collision data collected at $\sqrt{s} = 13\,\mathrm{TeV}$ with the CMS detector, corresponding to an integrated luminosity of $35.9\,\mathrm{fb}^{-1}$. The spectra obtained are based on data from the $\mathrm{H} \to \gamma\gamma$, $\mathrm{H} \to \mathrm{ZZ}$, and $\mathrm{H} \to \mathrm{b\bar{b}}$ decay channels. The precision of the combined measurement of the differential cross section of $p_{\mathrm{T}}^{\mathrm{H}}$ is improved by about 15% with respect to the $\mathrm{H} \to \gamma\gamma$ channel alone. The improvement is larger in the low-$p_{\mathrm{T}}^{\mathrm{H}}$ region than in the high-$p_{\mathrm{T}}^{\mathrm{H}}$ tails. No significant deviations from the standard model are observed in any differential distribution. Additionally, the total cross section for Higgs boson production based on a combination of the $\mathrm{H} \to \gamma\gamma$ and $\mathrm{H} \to \mathrm{ZZ}$ channels is measured to be $61.1 \pm 6.0\,(\mathrm{stat}) \pm 3.7\,(\mathrm{syst})\,\mathrm{pb}$.

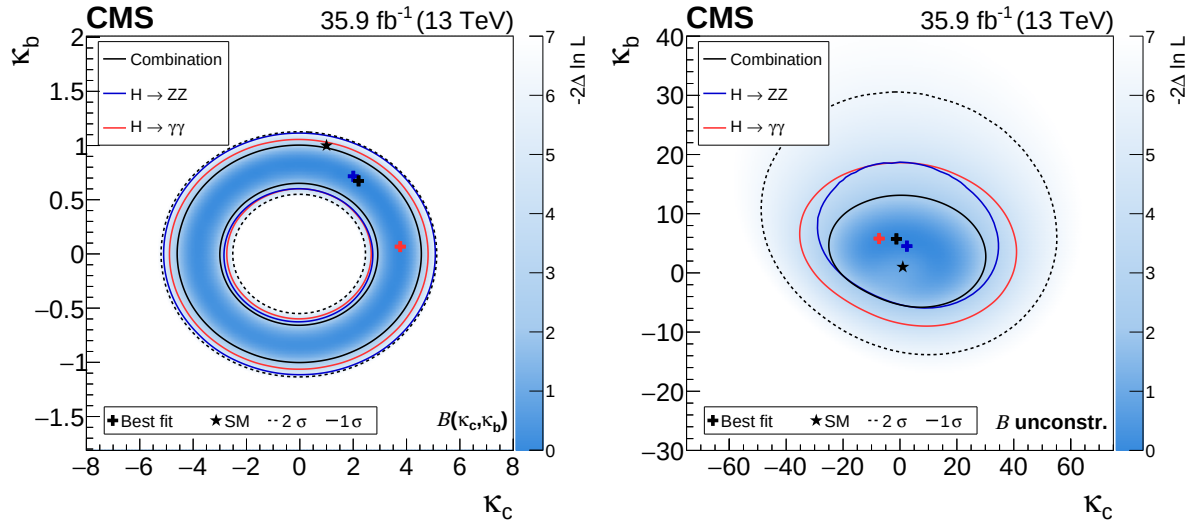

Figure 6: Simultaneous fit to data for κ_b and κ_c, assuming a coupling dependence of the branching fractions (left) and the branching fractions implemented as nuisance parameters with no prior constraint (right). The one standard deviation contour is drawn for the combination ($H \to \gamma\gamma$ and $H \to ZZ$), the $H \to \gamma\gamma$ channel, and the $H \to ZZ$ channel in black, red, and blue, respectively. For the combination the two standard deviation contour is drawn as a black dashed line, and the shading indicates the negative log-likelihood, with the scale shown on the right hand side of the plots.

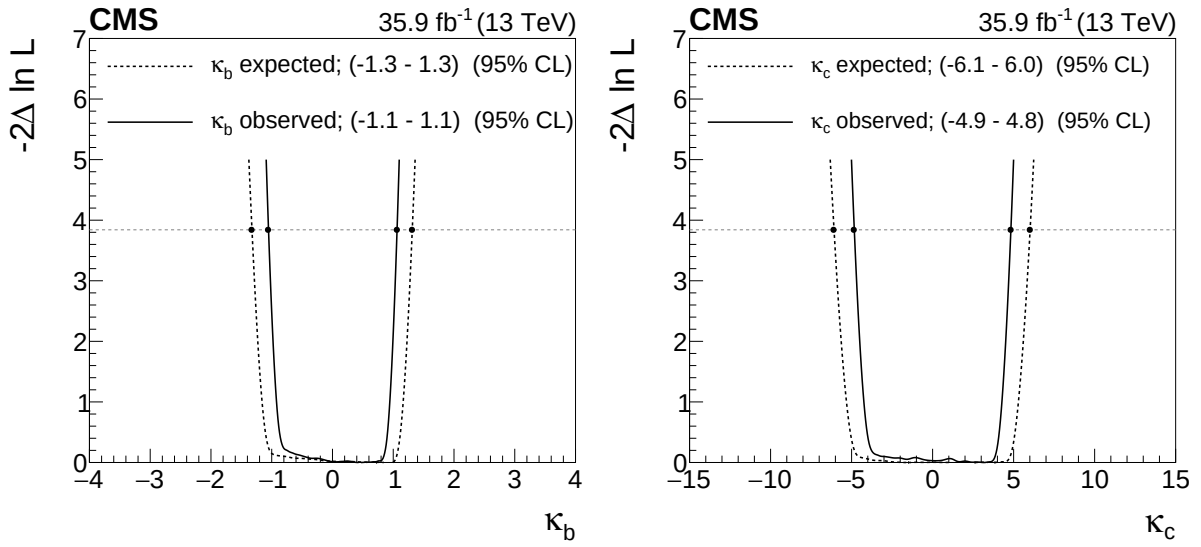

Figure 7: Likelihood scan of κ_b while profiling κ_c (left), and of κ_c while profiling κ_b (right). The filled markers indicate the limits at 95% CL. The branching fractions are considered dependent on the values of the couplings.

The spectra obtained are interpreted in the κ-framework [32], in which simultaneous variations of κ_b and κ_c, κ_t and κ_b, and κ_t and the anomalous direct coupling to the gluon field c_g are fitted to the p_T^H spectra. The limits obtained for the individual couplings are $-1.1 < \kappa_b < 1.1$ and $-4.9 < \kappa_c < 4.8$ at 95% confidence level, assuming the branching fractions scale with the Higgs boson couplings following the standard model prediction. For the charm coupling κ_c in

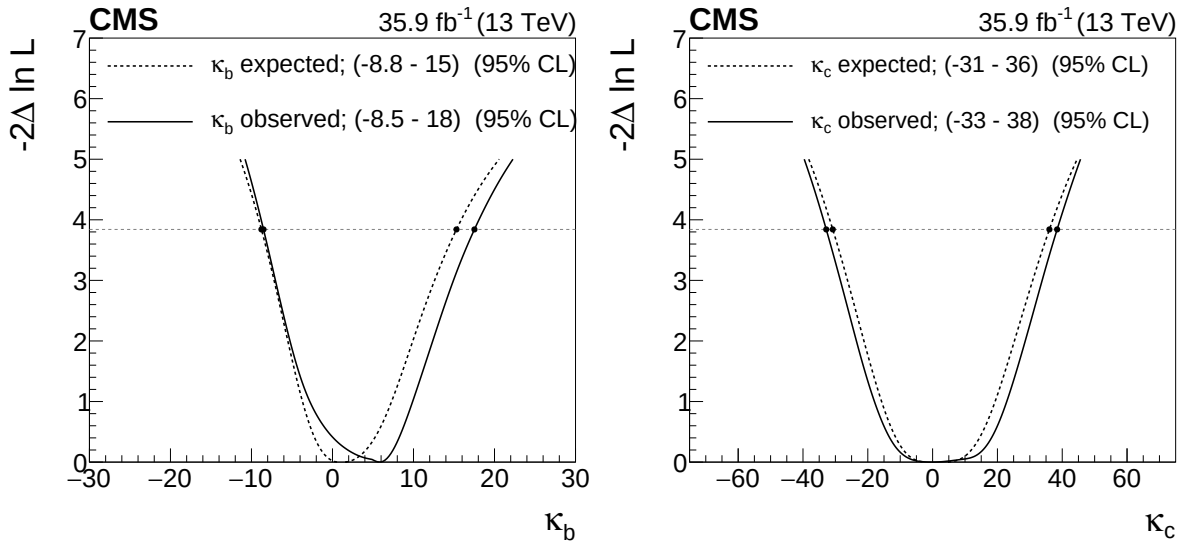

Figure 8: Likelihood scan of κ_b while profiling κ_c (left), and of κ_c while profiling κ_b (right). The filled markers indicate the limits at 95% CL. The branching fractions are implemented as nuisance parameters with no prior constraint.

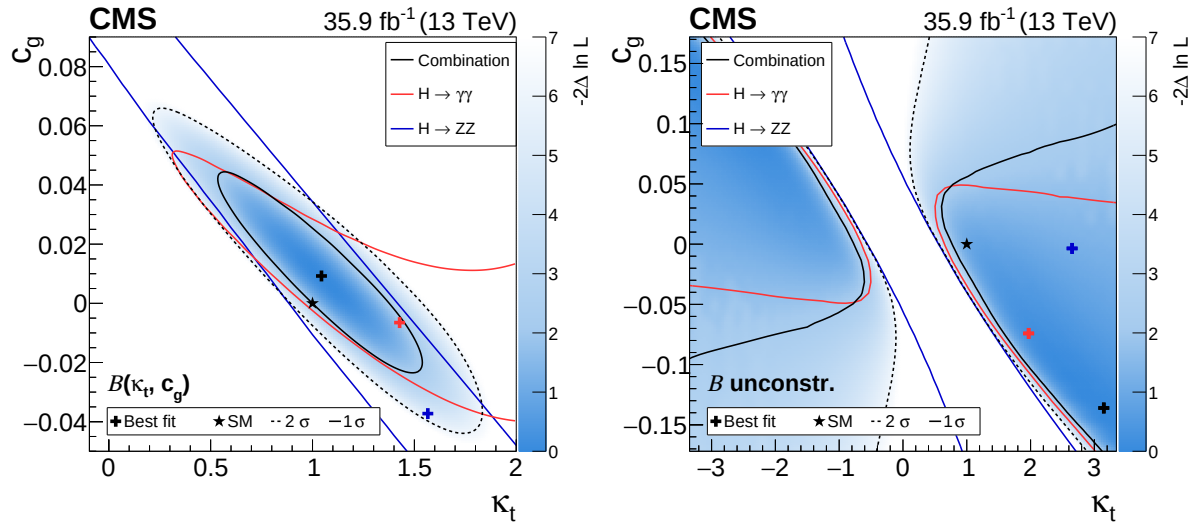

Figure 9: Simultaneous fit to data for κ_t and c_g, assuming a coupling dependence of the branching fractions (left) and the branching fractions implemented as nuisance parameters with no prior constraint (right). The one standard deviation contour is drawn for the combination ($H \to \gamma\gamma$, $H \to ZZ$, and $H \to b\bar{b}$), the $H \to \gamma\gamma$ channel, and the $H \to ZZ$ channel in black, red, and blue, respectively. For the combination the two standard deviation contour is drawn as a black dashed line, and the shading indicates the negative log-likelihood, with the scale shown on the right hand side of the plots.

particular, these bounds are comparable with those obtained from direct searches with charm quarks in the final state.

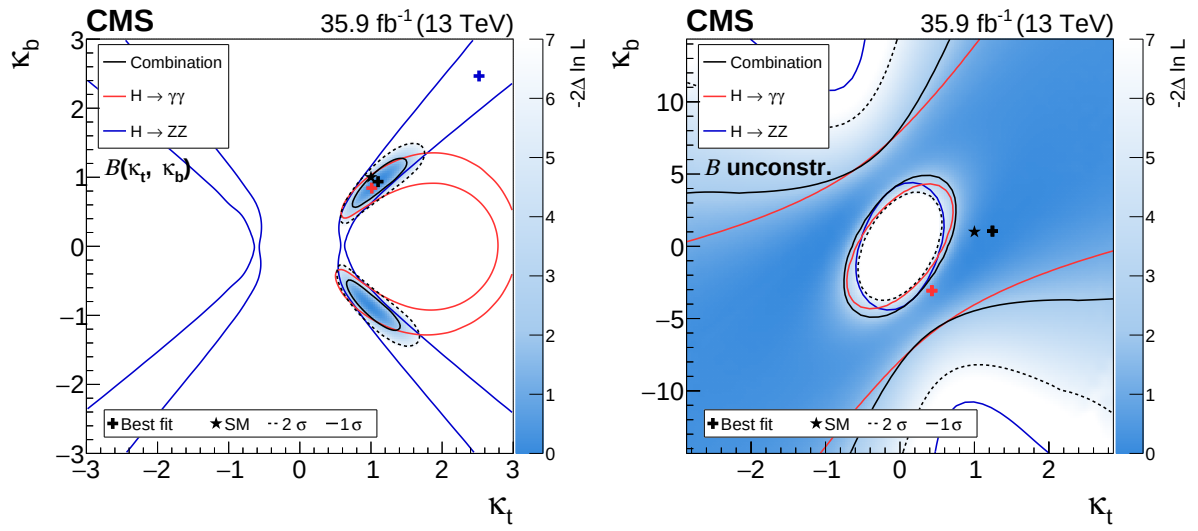

Figure 10: Simultaneous fit to data for κ_t and κ_b, assuming a coupling dependence of the branching fractions (left) and the branching fractions implemented as nuisance parameters with no prior constraint (right). The one standard deviation contour is drawn for the combination ($H \to \gamma\gamma$, $H \to ZZ$, and $H \to b\bar{b}$), the $H \to \gamma\gamma$ channel, and the $H \to ZZ$ channel in black, red, and blue, respectively. For the combination the two standard deviation contour is drawn as a black dashed line, and the shading indicates the negative log-likelihood, with the scale shown on the right hand side of the plots.

Acknowledgments

We thank Fady Bishara, Ulrich Haisch, Pier Francesco Monni, Emanuele Re, Massimiliano Grazzini, Agnieszka Ilnicka, Michael Spira, and Marius Wiesemann for guidance regarding their predictions of the Higgs boson transverse momentum spectra. We congratulate our colleagues in the CERN accelerator departments for the excellent performance of the LHC and thank the technical and administrative staffs at CERN and at other CMS institutes for their contributions to the success of the CMS effort. In addition, we gratefully acknowledge the computing centres and personnel of the Worldwide LHC Computing Grid for delivering so effectively the computing infrastructure essential to our analyses. Finally, we acknowledge the enduring support for the construction and operation of the LHC and the CMS detector provided by the following funding agencies: BMBWF and FWF (Austria); FNRS and FWO (Belgium); CNPq, CAPES, FAPERJ, FAPERGS, and FAPESP (Brazil); MES (Bulgaria); CERN; CAS, MoST, and NSFC (China); COLCIENCIAS (Colombia); MSES and CSF (Croatia); RPF (Cyprus); SENESCYT (Ecuador); MoER, ERC IUT, and ERDF (Estonia); Academy of Finland, MEC, and HIP (Finland); CEA and CNRS/IN2P3 (France); BMBF, DFG, and HGF (Germany); GSRT (Greece); NKFIA (Hungary); DAE and DST (India); IPM (Iran); SFI (Ireland); INFN (Italy); MSIP and NRF (Republic of Korea); MES (Latvia); LAS (Lithuania); MOE and UM (Malaysia); BUAP, CINVESTAV, CONACYT, LNS, SEP, and UASLP-FAI (Mexico); MOS (Montenegro); MBIE (New Zealand); PAEC (Pakistan); MSHE and NSC (Poland); FCT (Portugal); JINR (Dubna); MON, RosAtom, RAS, RFBR, and NRC KI (Russia); MESTD (Serbia); SEIDI, CPAN, PCTI, and FEDER (Spain); MOSTR (Sri Lanka); Swiss Funding Agencies (Switzerland); MST (Taipei); ThEPCenter, IPST, STAR, and NSTDA (Thailand); TUBITAK and TAEK (Turkey); NASU and SFFR (Ukraine); STFC (United Kingdom); DOE and NSF (USA).

Individuals have received support from the Marie-Curie programme and the European Re-

search Council and Horizon 2020 Grant, contract No. 675440 (European Union); the Leventis Foundation; the A.P. Sloan Foundation; the Alexander von Humboldt Foundation; the Belgian Federal Science Policy Office; the Fonds pour la Formation à la Recherche dans l'Industrie et dans l'Agriculture (FRIA-Belgium); the Agentschap voor Innovatie door Wetenschap en Technologie (IWT-Belgium); the F.R.S.-FNRS and FWO (Belgium) under the "Excellence of Science – EOS" – be.h project n. 30820817; the Ministry of Education, Youth and Sports (MEYS) of the Czech Republic; the Lendület ("Momentum") Programme and the János Bolyai Research Scholarship of the Hungarian Academy of Sciences, the New National Excellence Program ÚNKP, the NKFIA research grants 123842, 123959, 124845, 124850, and 125105 (Hungary); the Council of Science and Industrial Research, India; the HOMING PLUS programme of the Foundation for Polish Science, cofinanced from European Union, Regional Development Fund, the Mobility Plus programme of the Ministry of Science and Higher Education, the National Science Center (Poland), contracts Harmonia 2014/14/M/ST2/00428, Opus 2014/13/B/ST2/02543, 2014/15/B/ST2/03998, and 2015/19/B/ST2/02861, Sonata-bis 2012/07/E/ST2/01406; the National Priorities Research Program by Qatar National Research Fund; the Programa Estatal de Fomento de la Investigación Científica y Técnica de Excelencia María de Maeztu, grant MDM-2015-0509 and the Programa Severo Ochoa del Principado de Asturias; the Thalis and Aristeia programmes cofinanced by EU-ESF and the Greek NSRF; the Rachadapisek Sompot Fund for Postdoctoral Fellowship, Chulalongkorn University and the Chulalongkorn Academic into Its 2nd Century Project Advancement Project (Thailand); the Welch Foundation, contract C-1845; and the Weston Havens Foundation (USA).

References

[1] P. W. Higgs, "Broken symmetries and the masses of gauge bosons", *Phys. Rev. Lett.* **13** (1964) 508, doi:10.1103/PhysRevLett.13.508.

[2] F. Englert and R. Brout, "Broken symmetry and the mass of gauge vector mesons", *Phys. Rev. Lett.* **13** (1964) 321, doi:10.1103/PhysRevLett.13.321.

[3] G. S. Guralnik, C. R. Hagen, and T. W. B. Kibble, "Global conservation laws and massless particles", *Phys. Rev. Lett.* **13** (1964) 585, doi:10.1103/PhysRevLett.13.585.

[4] ATLAS Collaboration, "Observation of a new particle in the search for the standard model Higgs boson with the ATLAS detector at the LHC", *Phys. Lett. B* **716** (2012) 1, doi:10.1016/j.physletb.2012.08.020, arXiv:1207.7214.

[5] CMS Collaboration, "Observation of a new boson at a mass of 125 GeV with the CMS experiment at the LHC", *Phys. Lett. B* **716** (2012) 30, doi:10.1016/j.physletb.2012.08.021, arXiv:1207.7235.

[6] CMS Collaboration, "Observation of a new boson with mass near 125 GeV in pp collisions at $\sqrt{s}$ = 7 and 8 TeV", *JHEP* **06** (2013) 081, doi:10.1007/JHEP06(2013)081, arXiv:1303.4571.

[7] ATLAS and CMS Collaborations, "Measurements of the Higgs boson production and decay rates and constraints on its couplings from a combined ATLAS and CMS analysis of the LHC pp collision data at $\sqrt{s}$ = 7 and 8 TeV", *JHEP* **08** (2016) 045, doi:10.1007/JHEP08(2016)045, arXiv:1606.02266.

[8] ATLAS and CMS Collaborations, "Combined measurement of the Higgs boson mass in pp collisions at $\sqrt{s}$ = 7 and 8 TeV with the ATLAS and CMS experiments", *Phys. Rev. Lett.* **114** (2015) 191803, doi:10.1103/PhysRevLett.114.191803, arXiv:1503.07589.

[9] CMS Collaboration, "Combined measurements of Higgs boson couplings in proton-proton collisions at $\sqrt{s} = 13$ TeV", (2018). arXiv:1809.10733. Submitted to *Eur. Phys. J. C*.

[10] S. Dimopoulos and H. Georgi, "Softly broken supersymmetry and SU(5)", *Nucl. Phys. B* **193** (1981) 150, doi:10.1016/0550-3213(81)90522-8.

[11] E. Witten, "Dynamical breaking of supersymmetry", *Nucl. Phys. B* **188** (1981) 513, doi:10.1016/0550-3213(81)90006-7.

[12] F. Bishara, U. Haisch, P. F. Monni, and E. Re, "Constraining light-quark Yukawa couplings from Higgs distributions", *Phys. Rev. Lett.* **118** (2017) 121801, doi:10.1103/PhysRevLett.118.121801, arXiv:1606.09253.

[13] ATLAS Collaboration, "Measurements of the total and differential Higgs boson production cross sections combining the $H \to \gamma\gamma$ and $H \to ZZ \to 4\ell$ decay channels at $\sqrt{s}$ = 8 TeV with the ATLAS detector", *Phys. Rev. Lett.* **115** (2015) 091801, doi:10.1103/PhysRevLett.115.091801, arXiv:1504.05833.

[14] ATLAS Collaboration, "Search for Higgs and Z boson decays to $J/\psi\gamma$ and $\Upsilon(nS)\gamma$ with the ATLAS detector", *Phys. Rev. Lett.* **114** (2015) 121801, doi:10.1103/PhysRevLett.114.121801, arXiv:1501.03276.

[15] M. König and M. Neubert, "Exclusive radiative Higgs decays as probes of light-quark Yukawa couplings", *JHEP* **08** (2015) 012, doi:10.1007/JHEP08(2015)012, arXiv:1505.03870.

[16] ATLAS Collaboration, "Searches for exclusive Higgs and Z boson decays into $J/\psi\gamma$, $\psi(2S)\gamma$, and $\Upsilon(nS)\gamma$ at $\sqrt{s} = 13$ TeV with the ATLAS detector", *Phys. Lett. B* **786** (2018) 134, doi:10.1016/j.physletb.2018.09.024, arXiv:1807.00802.

[17] ATLAS Collaboration, "Search for the decay of the Higgs boson to charm quarks with the ATLAS experiment", *Phys. Rev. Lett.* **120** (2018) 211802, doi:10.1103/PhysRevLett.120.211802, arXiv:1802.04329.

[18] ATLAS Collaboration, "Measurements of fiducial and differential cross sections for Higgs boson production in the diphoton decay channel at $\sqrt{s}$ = 8 TeV with ATLAS", *JHEP* **09** (2014) 112, doi:10.1007/JHEP09(2014)112, arXiv:1407.4222.

[19] CMS Collaboration, "Measurement of differential cross sections for Higgs boson production in the diphoton decay channel in pp collisions at $\sqrt{s}$ = 8 TeV", *Eur. Phys. J. C* **76** (2016) 13, doi:10.1140/epjc/s10052-015-3853-3, arXiv:1508.07819.

[20] ATLAS Collaboration, "Fiducial and differential cross sections of Higgs boson production measured in the four-lepton decay channel in pp collisions at $\sqrt{s}$ = 8 TeV with the ATLAS detector", *Phys. Lett. B* **738** (2014) 234, doi:10.1016/j.physletb.2014.09.054, arXiv:1408.3226.

[21] CMS Collaboration, "Measurement of differential and integrated fiducial cross sections for Higgs boson production in the four-lepton decay channel in pp collisions at $\sqrt{s}$ = 7 and 8 TeV", *JHEP* **04** (2016) 005, doi:10.1007/JHEP04(2016)005, arXiv:1512.08377.

[22] ATLAS Collaboration, "Measurement of fiducial differential cross sections of gluon-fusion production of Higgs bosons decaying to $WW^* \to e\nu\mu\nu$ with the ATLAS detector at $\sqrt{s}$ = 8 TeV", *JHEP* **08** (2016) 104, doi:10.1007/JHEP08(2016)104, arXiv:1604.02997.

[23] CMS Collaboration, "Measurement of the transverse momentum spectrum of the Higgs boson produced in pp collisions at $\sqrt{s}$ = 8 TeV using $H \to WW$ decays", *JHEP* **03** (2017) 032, doi:10.1007/JHEP03(2017)032, arXiv:1606.01522.

[24] ATLAS Collaboration, "Measurements of Higgs boson properties in the diphoton decay channel with 36 fb^{-1} of pp collision data at $\sqrt{s} = 13$ TeV with the ATLAS detector", *Phys. Rev. D* **98** (2018) 052005, doi:10.1103/PhysRevD.98.052005, arXiv:1802.04146.

[25] CMS Collaboration, "Measurement of inclusive and differential Higgs boson production cross sections in the diphoton decay channel in proton-proton collisions at $\sqrt{s} = 13$ TeV", *JHEP* **01** (2019) 183, doi:10.1007/JHEP01(2019)183, arXiv:1807.03825.

[26] ATLAS Collaboration, "Measurement of inclusive and differential cross sections in the $H \to ZZ^* \to 4\ell$ decay channel in pp collisions at $\sqrt{s}$ = 13 TeV with the ATLAS detector", *JHEP* **10** (2017) 132, doi:10.1007/JHEP10(2017)132, arXiv:1708.02810.

[27] CMS Collaboration, "Measurements of properties of the Higgs boson decaying into the four-lepton final state in pp collisions at $\sqrt{s}$ = 13 TeV", *JHEP* **11** (2017) 047, doi:10.1007/JHEP11(2017)047, arXiv:1706.09936.

[28] ATLAS Collaboration, "Combined measurement of differential and total cross sections in the $H \to \gamma\gamma$ and the $H \to ZZ^* \to 4\ell$ decay channels at $\sqrt{s} = 13$ TeV with the ATLAS detector", *Phys. Lett. B* **786** (2018) 114, doi:10.1016/j.physletb.2018.09.019, arXiv:1805.10197.

[29] CMS Collaboration, "Inclusive search for a highly boosted Higgs boson decaying to a bottom quark-antiquark pair", *Phys. Rev. Lett.* **120** (2018) 071802, doi:10.1103/PhysRevLett.120.071802, arXiv:1709.05543.

[30] M. Grazzini, A. Ilnicka, M. Spira, and M. Wiesemann, "Effective field theory for Higgs properties parametrisation: The transverse momentum spectrum case", in *Proceedings, 52nd Rencontres de Moriond on QCD and High Energy Interactions: La Thuile, Italy, March 25-April 1, 2017*, p. 23. 2017. arXiv:1705.05143.

[31] M. Grazzini, A. Ilnicka, M. Spira, and M. Wiesemann, "Modeling BSM effects on the Higgs transverse-momentum spectrum in an EFT approach", *JHEP* **03** (2017) 115, doi:10.1007/JHEP03(2017)115, arXiv:1612.00283.

[32] LHC Higgs Cross Section Working Group, "Handbook of LHC Higgs cross sections: 3. Higgs properties", *CERN* (2013) doi:10.5170/CERN-2013-004, arXiv:1307.1347.

[33] A. Banfi, P. F. Monni, and G. Zanderighi, "Quark masses in Higgs production with a jet veto", *JHEP* **01** (2014) 097, doi:10.1007/JHEP01(2014)097, arXiv:1308.4634.

[34] G. Bozzi, S. Catani, D. de Florian, and M. Grazzini, "The q_{T} spectrum of the Higgs boson at the LHC in QCD perturbation theory", *Phys. Lett. B* **564** (2003) 65, doi:10.1016/S0370-2693(03)00656-7, arXiv:hep-ph/0302104.

[35] T. Becher and M. Neubert, "Drell-Yan production at small q_{T}, transverse parton distributions and the collinear anomaly", *Eur. Phys. J. C* **71** (2011) 1665, doi:10.1140/epjc/s10052-011-1665-7, arXiv:1007.4005.

[36] P. F. Monni, E. Re, and P. Torrielli, "Higgs transverse-momentum resummation in direct space", *Phys. Rev. Lett.* **116** (2016) 242001, doi:10.1103/PhysRevLett.116.242001, arXiv:1604.02191.

[37] CMS Collaboration, "The CMS experiment at the CERN LHC", *JINST* **3** (2008) S08004, doi:10.1088/1748-0221/3/08/S08004.

[38] J. Alwall et al., "The automated computation of tree-level and next-to-leading order differential cross sections, and their matching to parton shower simulations", *JHEP* **07** (2014) 079, doi:10.1007/JHEP07(2014)079, arXiv:1405.0301.

[39] T. Sjöstrand et al., "An introduction to PYTHIA 8.2", *Comput. Phys. Commun.* **191** (2015) 159, doi:10.1016/j.cpc.2015.01.024, arXiv:1410.3012.

[40] P. Skands, S. Carrazza, and J. Rojo, "Tuning PYTHIA 8.1: the Monash 2013 tune", *Eur. Phys. J. C* **74** (2014) 3024, doi:10.1140/epjc/s10052-014-3024-y, arXiv:1404.5630.

[41] R. Frederix and S. Frixione, "Merging meets matching in MC@NLO", *JHEP* **12** (2012) 061, doi:10.1007/JHEP12(2012)061, arXiv:1209.6215.

[42] K. Hamilton, P. Nason, and G. Zanderighi, "MINLO: Multi-scale improved NLO", *JHEP* **10** (2012) 155, doi:10.1007/JHEP10(2012)155, arXiv:1206.3572.

[43] A. Kardos, P. Nason, and C. Oleari, "Three-jet production in POWHEG", *JHEP* **04** (2014) 043, doi:10.1007/JHEP04(2014)043, arXiv:1402.4001.

[44] NNPDF Collaboration, "Parton distributions for the LHC Run II", *JHEP* **04** (2015) 040, doi:10.1007/JHEP04(2015)040, arXiv:1410.8849.

[45] CMS Collaboration, "Particle-flow reconstruction and global event description with the CMS detector", *JINST* **12** (2017) P10003, doi:10.1088/1748-0221/12/10/P10003, arXiv:1706.04965.

[46] M. Cacciari, G. P. Salam, and G. Soyez, "The anti-k_{T} jet clustering algorithm", *JHEP* **04** (2008) 063, doi:10.1088/1126-6708/2008/04/063, arXiv:0802.1189.

[47] M. Dasgupta, A. Fregoso, S. Marzani, and G. P. Salam, "Towards an understanding of jet substructure", *JHEP* **09** (2013) 029, doi:10.1007/JHEP09(2013)029, arXiv:1307.0007.

[48] A. J. Larkoski, S. Marzani, G. Soyez, and J. Thaler, "Soft drop", *JHEP* **05** (2014) 146, doi:10.1007/JHEP05(2014)146, arXiv:1402.2657.

[49] J. Dolen et al., "Thinking outside the ROCs: Designing decorrelated taggers (DDT) for jet substructure", *JHEP* **05** (2016) 156, doi:10.1007/JHEP05(2016)156, arXiv:1603.00027.

[50] I. Moult, L. Necib, and J. Thaler, "New angles on energy correlation functions", *JHEP* **12** (2016) 153, doi:10.1007/JHEP12(2016)153, arXiv:1609.07483.

[51] A. J. Larkoski, G. P. Salam, and J. Thaler, "Energy correlation functions for jet substructure", *JHEP* **06** (2013) 108, doi:10.1007/JHEP06(2013)108, arXiv:1305.0007.

[52] J. Thaler and K. Van Tilburg, "Identifying boosted objects with N-subjettiness", *JHEP* **03** (2011) 015, doi:10.1007/JHEP03(2011)015, arXiv:1011.2268.

[53] CMS Collaboration, "Identification of heavy-flavour jets with the CMS detector in pp collisions at 13 TeV", *JINST* **13** (2018) P05011, doi:10.1088/1748-0221/13/05/P05011, arXiv:1712.07158.

[54] P. C. Hansen, "The L-curve and its use in the numerical treatment of inverse problems", in *Computational Inverse Problems in Electrocardiology*, p. 119. Southampton: WIT Press, 2001.

[55] G. Cowan, K. Cranmer, E. Gross, and O. Vitells, "Asymptotic formulae for likelihood-based tests of new physics", *Eur. Phys. J. C* **71** (2011) 1554, doi:10.1140/epjc/s10052-011-1554-0, arXiv:1007.1727. [Erratum: doi:10.1140/epjc/s10052-013-2501-z].

[56] The ATLAS Collaboration, The CMS Collaboration, The LHC Higgs Combination Group, "Procedure for the LHC Higgs boson search combination in Summer 2011", Technical Report CMS-NOTE-2011-005, ATL-PHYS-PUB-2011-11, 2011.

[57] LHC Higgs Cross Section Working Group, "Handbook of LHC Higgs cross sections: 4. Deciphering the nature of the Higgs sector", *CERN* (2016) doi:10.23731/CYRM-2017-002, arXiv:1610.07922.

A Tables for the differential cross section measurements

Tables A.1–A.5 show the measured differential cross sections for the considered observables.

Table A.1: Differential cross sections (pb/GeV) for the observable $p_{\mathrm{T}}^{\mathrm{H}}$.

$p_{\mathrm{T}}^{\mathrm{H}}$ (GeV)	0–15	15–30	30–45	45–80	80–120	120–200	200–350	350–600	>600
$\mathrm{H} \to \gamma\gamma$	$1.0^{+0.3}_{-0.3}$	$1^{+0.3}_{-0.3}$	$0.5^{+0.2}_{-0.2}$	$0.3^{+0.1}_{-0.1}$	$0.1^{+0.05}_{-0.05}$	$0.03^{+0.01}_{-0.01}$	$0.01^{+2.8\times10^{-3}}_{-2.5\times10^{-3}}$	$-3.4\times10^{-5}\,^{+3.8\times10^{-4}}_{-3.1\times10^{-4}}$	$-1.9\times10^{-4}\,^{+2.4\times10^{-4}}_{-2.4\times10^{-4}}$
$\mathrm{H} \to \mathrm{ZZ}$	$0.7^{+0.3}_{-0.3}$	$1^{+0.4}_{-0.3}$	$0.4^{+0.1}_{-0.1}$		$0.08^{+0.03}_{-0.02}$		$3.3\times10^{-4}\,^{+2.6\times10^{-3}}_{-2.6\times10^{-3}}$		
$\mathrm{H} \to \mathrm{b\bar{b}}$	*None*							$9.6\times10^{-4}\,^{+1.2\times10^{-3}}_{-1.2\times10^{-3}}$	$1.1\times10^{-4}\,^{+1.2\times10^{-4}}_{-1.1\times10^{-4}}$
Comb.	$0.8^{+0.2}_{-0.2}$	$1^{+0.2}_{-0.3}$	$0.6^{+0.2}_{-0.2}$	$0.3^{+0.1}_{-0.09}$	$0.1^{+0.05}_{-0.04}$	$0.03^{+0.01}_{-0.01}$	$0.01^{+2.6\times10^{-3}}_{-2.4\times10^{-3}}$	$-2.8\times10^{-6}\,^{+3.7\times10^{-4}}_{-2.8\times10^{-4}}$	$5.8\times10^{-5}\,^{+1.0\times10^{-4}}_{-1.0\times10^{-4}}$

Table A.2: Differential cross sections of gluon fusion (ggH) (pb/GeV) for the observable $p_{\mathrm{T}}^{\mathrm{H}}$, with non-ggH production modes fixed to their SM prediction.

$p_{\mathrm{T}}^{\mathrm{H}}$ (GeV)	0–15	15–30	30–45	45–80	80–120	120–200	200–350	350–600	>600
Comb.	$0.8^{+0.2}_{-0.2}$	$1^{+0.2}_{-0.3}$	$0.5^{+0.2}_{-0.2}$	$0.2^{+0.1}_{-0.09}$	$0.1^{+0.05}_{-0.04}$	$0.02^{+0.01}_{-0.01}$	$8.3\times10^{-3}\,^{+2.6\times10^{-3}}_{-2.4\times10^{-3}}$	$-1.6\times10^{-4}\,^{+3.4\times10^{-4}}_{-2.6\times10^{-4}}$	$3.5\times10^{-5}\,^{+5.8\times10^{-5}}_{-5.7\times10^{-5}}$

Table A.3: Differential cross sections (pb) for the observable N_{jets}.

N_{jets}	0	1	2	3	$\geq$4
$\mathrm{H} \to \gamma\gamma$	$50^{+8.5}_{-8.1}$	$14^{+5.1}_{-4.9}$	$4.8\times10^{-1}\,^{+2.7}_{-2.7}$	$3.1^{+2.0}_{-2.0}$	$1.3\,^{+8.8\times10^{-1}}_{-9.3\times10^{-1}}$
$\mathrm{H} \to \mathrm{ZZ}$	$41^{+9.1}_{-8.0}$	$8.7^{+5.2}_{-4.3}$	$6.9^{+3.7}_{-3.0}$	$1.2^{+2.1}_{-2.1}$	
Combination	$47^{+6.2}_{-6.4}$	$11^{+3.7}_{-3.4}$	$3.5^{+1.9}_{-1.7}$	$1.8^{+1.7}_{-1.5}$	$1.2\,^{+8.3\times10^{-1}}_{-8.8\times10^{-1}}$

Table A.4: Differential cross sections (pb) for the observable $|y_{\mathrm{H}}|$.

$\lvert y_{\mathrm{H}}\rvert$	0–0.15	0.15–0.3	0.3–0.6	0.6–0.9	0.9–1.2	1.2–2.5
$\mathrm{H} \to \gamma\gamma$	42^{+11}_{-11}	39^{+12}_{-11}	$31^{+9.0}_{-7.5}$	$28^{+9.1}_{-8.7}$	24^{+12}_{-10}	$18^{+7.4}_{-7.2}$
$\mathrm{H} \to \mathrm{ZZ}$	39^{+17}_{-14}	35^{+18}_{-14}	$34^{+11}_{-9.8}$	45^{+13}_{-11}	$13^{+8.9}_{-6.8}$	$13^{+6.7}_{-5.4}$
Combination	$41^{+9.1}_{-8.9}$	$38^{+9.7}_{-9.2}$	$32^{+7.0}_{-6.0}$	$35^{+7.1}_{-6.6}$	$17^{+7.4}_{-6.5}$	$15^{+5.1}_{-4.7}$

Table A.5: Differential cross sections (pb/GeV) for the observable $p_{\mathrm{T}}^{\mathrm{jet}}$.

$p_{\mathrm{T}}^{\mathrm{jet}}$ (GeV)	30–55	55–95	95–120	120–200	>200
$\mathrm{H} \to \gamma\gamma$	$1.6\times10^{-1}\,^{+2.0\times10^{-1}}_{-2.1\times10^{-1}}$	$2.0\times10^{-1}\,^{+9.2\times10^{-2}}_{-9.3\times10^{-2}}$	$1.3\times10^{-1}\,^{+9.5\times10^{-2}}_{-9.2\times10^{-2}}$	$1.5\times10^{-5}\,^{+1.8\times10^{-2}}_{-1.7\times10^{-2}}$	$2.9\times10^{-2}\,^{+9.1\times10^{-3}}_{-9.2\times10^{-3}}$
$\mathrm{H} \to \mathrm{ZZ}$	$4.8\times10^{-1}\,^{+2.4\times10^{-1}}_{-2.0\times10^{-1}}$	$7.7\times10^{-2}\,^{+8.8\times10^{-2}}_{-6.9\times10^{-2}}$	$8.0\times10^{-2}\,^{+5.9\times10^{-2}}_{-4.4\times10^{-2}}$		
Combination	$3.2\times10^{-1}\,^{+1.4\times10^{-1}}_{-1.3\times10^{-1}}$	$1.3\times10^{-1}\,^{+7.7\times10^{-2}}_{-6.1\times10^{-2}}$	$1.1\times10^{-1}\,^{+8.4\times10^{-2}}_{-8.1\times10^{-2}}$	$-4.2\times10^{-3}\,^{+1.7\times10^{-2}}_{-1.6\times10^{-2}}$	$2.7\times10^{-2}\,^{+8.7\times10^{-3}}_{-8.9\times10^{-3}}$

B Correlation matrices for the combinations of differential observables

Figs. B.1–B.4 show the correlation matrices for the considered observables.

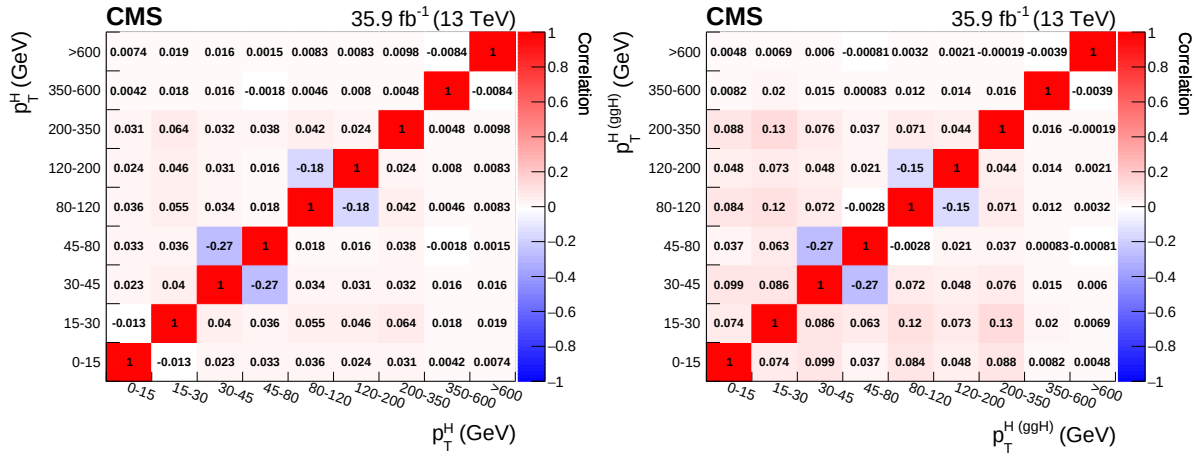

Figure B.1: Bin-to-bin correlation matrix of the $p_{\mathrm{T}}^{\mathrm{H}}$ spectrum (left) and of the $p_{\mathrm{T}}^{\mathrm{H}}$ spectrum of gluon fusion (ggH), where the non-ggH contributions are fixed to the SM expectation (right).

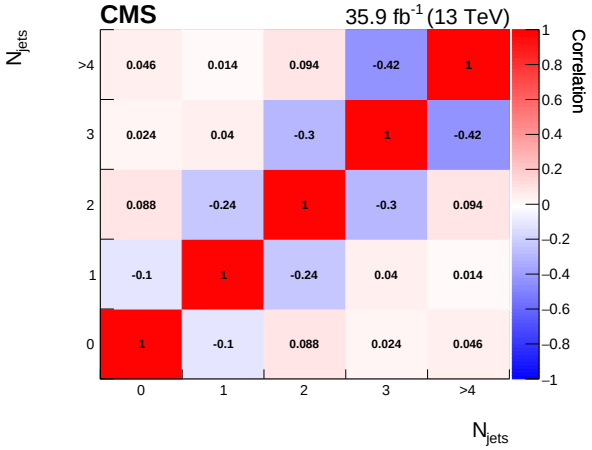

Figure B.2: Bin-to-bin correlation matrix of the N_{jets} spectrum.

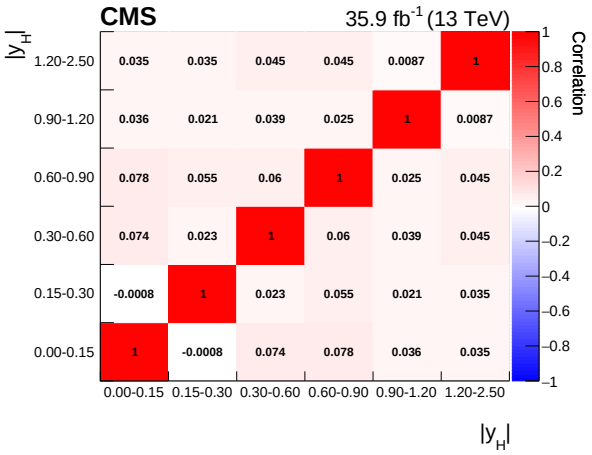

Figure B.3: Bin-to-bin correlation matrix of the $|y_{\mathrm{H}}|$ spectrum.

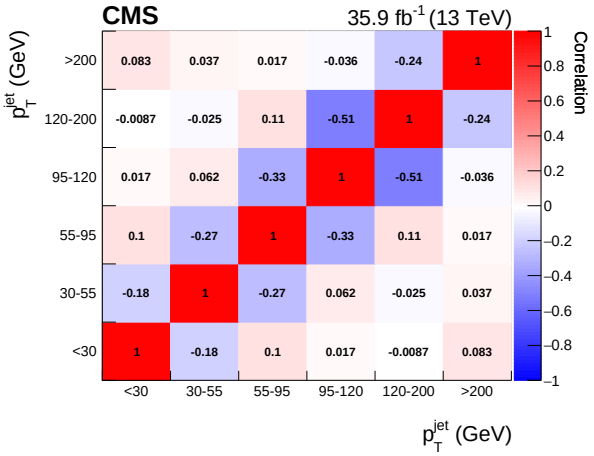

Figure B.4: Bin-to-bin correlation matrix of the $p_{\mathrm{T}}^{\mathrm{jet}}$ spectrum.

C The CMS Collaboration

Yerevan Physics Institute, Yerevan, Armenia
A.M. Sirunyan, A. Tumasyan

Institut für Hochenergiephysik, Wien, Austria
W. Adam, F. Ambrogi, E. Asilar, T. Bergauer, J. Brandstetter, M. Dragicevic, J. Erö, A. Escalante Del Valle, M. Flechl, R. Frühwirth[1], V.M. Ghete, J. Hrubec, M. Jeitler[1], N. Krammer, I. Krätschmer, D. Liko, T. Madlener, I. Mikulec, N. Rad, H. Rohringer, J. Schieck[1], R. Schöfbeck, M. Spanring, D. Spitzbart, A. Taurok, W. Waltenberger, J. Wittmann, C.-E. Wulz[1], M. Zarucki

Institute for Nuclear Problems, Minsk, Belarus
V. Chekhovsky, V. Mossolov, J. Suarez Gonzalez

Universiteit Antwerpen, Antwerpen, Belgium
E.A. De Wolf, D. Di Croce, X. Janssen, J. Lauwers, M. Pieters, H. Van Haevermaet, P. Van Mechelen, N. Van Remortel

Vrije Universiteit Brussel, Brussel, Belgium
S. Abu Zeid, F. Blekman, J. D'Hondt, J. De Clercq, K. Deroover, G. Flouris, D. Lontkovskyi, S. Lowette, I. Marchesini, S. Moortgat, L. Moreels, Q. Python, K. Skovpen, S. Tavernier, W. Van Doninck, P. Van Mulders, I. Van Parijs

Université Libre de Bruxelles, Bruxelles, Belgium
D. Beghin, B. Bilin, H. Brun, B. Clerbaux, G. De Lentdecker, H. Delannoy, B. Dorney, G. Fasanella, L. Favart, R. Goldouzian, A. Grebenyuk, A.K. Kalsi, T. Lenzi, J. Luetic, N. Postiau, E. Starling, L. Thomas, C. Vander Velde, P. Vanlaer, D. Vannerom, Q. Wang

Ghent University, Ghent, Belgium
T. Cornelis, D. Dobur, A. Fagot, M. Gul, I. Khvastunov[2], D. Poyraz, C. Roskas, D. Trocino, M. Tytgat, W. Verbeke, B. Vermassen, M. Vit, N. Zaganidis

Université Catholique de Louvain, Louvain-la-Neuve, Belgium
H. Bakhshiansohi, O. Bondu, S. Brochet, G. Bruno, C. Caputo, P. David, C. Delaere, M. Delcourt, A. Giammanco, G. Krintiras, V. Lemaitre, A. Magitteri, K. Piotrzkowski, A. Saggio, M. Vidal Marono, S. Wertz, J. Zobec

Centro Brasileiro de Pesquisas Fisicas, Rio de Janeiro, Brazil
F.L. Alves, G.A. Alves, M. Correa Martins Junior, G. Correia Silva, C. Hensel, A. Moraes, M.E. Pol, P. Rebello Teles

Universidade do Estado do Rio de Janeiro, Rio de Janeiro, Brazil
E. Belchior Batista Das Chagas, W. Carvalho, J. Chinellato[3], E. Coelho, E.M. Da Costa, G.G. Da Silveira[4], D. De Jesus Damiao, C. De Oliveira Martins, S. Fonseca De Souza, H. Malbouisson, D. Matos Figueiredo, M. Melo De Almeida, C. Mora Herrera, L. Mundim, H. Nogima, W.L. Prado Da Silva, L.J. Sanchez Rosas, A. Santoro, A. Sznajder, M. Thiel, E.J. Tonelli Manganote[3], F. Torres Da Silva De Araujo, A. Vilela Pereira

Universidade Estadual Paulista [a], Universidade Federal do ABC [b], São Paulo, Brazil
S. Ahuja[a], C.A. Bernardes[a], L. Calligaris[a], T.R. Fernandez Perez Tomei[a], E.M. Gregores[b], P.G. Mercadante[b], S.F. Novaes[a], SandraS. Padula[a]

Institute for Nuclear Research and Nuclear Energy, Bulgarian Academy of Sciences, Sofia,

Bulgaria
A. Aleksandrov, R. Hadjiiska, P. Iaydjiev, A. Marinov, M. Misheva, M. Rodozov, M. Shopova, G. Sultanov

University of Sofia, Sofia, Bulgaria
A. Dimitrov, L. Litov, B. Pavlov, P. Petkov

Beihang University, Beijing, China
W. Fang[5], X. Gao[5], L. Yuan

Institute of High Energy Physics, Beijing, China
M. Ahmad, J.G. Bian, G.M. Chen, H.S. Chen, M. Chen, Y. Chen, C.H. Jiang, D. Leggat, H. Liao, Z. Liu, F. Romeo, S.M. Shaheen[6], A. Spiezia, J. Tao, Z. Wang, E. Yazgan, H. Zhang, S. Zhang[6], J. Zhao

State Key Laboratory of Nuclear Physics and Technology, Peking University, Beijing, China
Y. Ban, G. Chen, A. Levin, J. Li, L. Li, Q. Li, Y. Mao, S.J. Qian, D. Wang

Tsinghua University, Beijing, China
Y. Wang

Universidad de Los Andes, Bogota, Colombia
C. Avila, A. Cabrera, C.A. Carrillo Montoya, L.F. Chaparro Sierra, C. Florez, C.F. González Hernández, M.A. Segura Delgado

University of Split, Faculty of Electrical Engineering, Mechanical Engineering and Naval Architecture, Split, Croatia
B. Courbon, N. Godinovic, D. Lelas, I. Puljak, T. Sculac

University of Split, Faculty of Science, Split, Croatia
Z. Antunovic, M. Kovac

Institute Rudjer Boskovic, Zagreb, Croatia
V. Brigljevic, D. Ferencek, K. Kadija, B. Mesic, A. Starodumov[7], T. Susa

University of Cyprus, Nicosia, Cyprus
M.W. Ather, A. Attikis, M. Kolosova, G. Mavromanolakis, J. Mousa, C. Nicolaou, F. Ptochos, P.A. Razis, H. Rykaczewski

Charles University, Prague, Czech Republic
M. Finger[8], M. Finger Jr.[8]

Escuela Politecnica Nacional, Quito, Ecuador
E. Ayala

Universidad San Francisco de Quito, Quito, Ecuador
E. Carrera Jarrin

Academy of Scientific Research and Technology of the Arab Republic of Egypt, Egyptian Network of High Energy Physics, Cairo, Egypt
H. Abdalla[9], A.A. Abdelalim[10,11], A. Mohamed[11]

National Institute of Chemical Physics and Biophysics, Tallinn, Estonia
S. Bhowmik, A. Carvalho Antunes De Oliveira, R.K. Dewanjee, K. Ehataht, M. Kadastik, M. Raidal, C. Veelken

Department of Physics, University of Helsinki, Helsinki, Finland
P. Eerola, H. Kirschenmann, J. Pekkanen, M. Voutilainen

Helsinki Institute of Physics, Helsinki, Finland
J. Havukainen, J.K. Heikkilä, T. Järvinen, V. Karimäki, R. Kinnunen, T. Lampén, K. Lassila-Perini, S. Laurila, S. Lehti, T. Lindén, P. Luukka, T. Mäenpää, H. Siikonen, E. Tuominen, J. Tuominiemi

Lappeenranta University of Technology, Lappeenranta, Finland
T. Tuuva

IRFU, CEA, Université Paris-Saclay, Gif-sur-Yvette, France
M. Besancon, F. Couderc, M. Dejardin, D. Denegri, J.L. Faure, F. Ferri, S. Ganjour, A. Givernaud, P. Gras, G. Hamel de Monchenault, P. Jarry, C. Leloup, E. Locci, J. Malcles, G. Negro, J. Rander, A. Rosowsky, M.Ö. Sahin, M. Titov

Laboratoire Leprince-Ringuet, Ecole polytechnique, CNRS/IN2P3, Université Paris-Saclay, Palaiseau, France
A. Abdulsalam[12], C. Amendola, I. Antropov, F. Beaudette, P. Busson, C. Charlot, R. Granier de Cassagnac, I. Kucher, A. Lobanov, J. Martin Blanco, C. Martin Perez, M. Nguyen, C. Ochando, G. Ortona, P. Paganini, P. Pigard, J. Rembser, R. Salerno, J.B. Sauvan, Y. Sirois, A.G. Stahl Leiton, A. Zabi, A. Zghiche

Université de Strasbourg, CNRS, IPHC UMR 7178, Strasbourg, France
J.-L. Agram[13], J. Andrea, D. Bloch, J.-M. Brom, E.C. Chabert, V. Cherepanov, C. Collard, E. Conte[13], J.-C. Fontaine[13], D. Gelé, U. Goerlach, M. Jansová, A.-C. Le Bihan, N. Tonon, P. Van Hove

Centre de Calcul de l'Institut National de Physique Nucleaire et de Physique des Particules, CNRS/IN2P3, Villeurbanne, France
S. Gadrat

Université de Lyon, Université Claude Bernard Lyon 1, CNRS-IN2P3, Institut de Physique Nucléaire de Lyon, Villeurbanne, France
S. Beauceron, C. Bernet, G. Boudoul, N. Chanon, R. Chierici, D. Contardo, P. Depasse, H. El Mamouni, J. Fay, L. Finco, S. Gascon, M. Gouzevitch, G. Grenier, B. Ille, F. Lagarde, I.B. Laktineh, H. Lattaud, M. Lethuillier, L. Mirabito, S. Perries, A. Popov[14], V. Sordini, G. Touquet, M. Vander Donckt, S. Viret

Georgian Technical University, Tbilisi, Georgia
A. Khvedelidze[8]

Tbilisi State University, Tbilisi, Georgia
Z. Tsamalaidze[8]

RWTH Aachen University, I. Physikalisches Institut, Aachen, Germany
C. Autermann, L. Feld, M.K. Kiesel, K. Klein, M. Lipinski, M. Preuten, M.P. Rauch, C. Schomakers, J. Schulz, M. Teroerde, B. Wittmer

RWTH Aachen University, III. Physikalisches Institut A, Aachen, Germany
A. Albert, D. Duchardt, M. Erdmann, S. Erdweg, T. Esch, R. Fischer, S. Ghosh, A. Güth, T. Hebbeker, C. Heidemann, K. Hoepfner, H. Keller, L. Mastrolorenzo, M. Merschmeyer, A. Meyer, P. Millet, S. Mukherjee, T. Pook, M. Radziej, H. Reithler, M. Rieger, A. Schmidt, D. Teyssier, S. Thüer

RWTH Aachen University, III. Physikalisches Institut B, Aachen, Germany
G. Flügge, O. Hlushchenko, T. Kress, T. Müller, A. Nehrkorn, A. Nowack, C. Pistone, O. Pooth, D. Roy, H. Sert, A. Stahl[15]

Deutsches Elektronen-Synchrotron, Hamburg, Germany
M. Aldaya Martin, T. Arndt, C. Asawatangtrakuldee, I. Babounikau, K. Beernaert, O. Behnke, U. Behrens, A. Bermúdez Martínez, D. Bertsche, A.A. Bin Anuar, K. Borras[16], V. Botta, A. Campbell, P. Connor, C. Contreras-Campana, V. Danilov, A. De Wit, M.M. Defranchis, C. Diez Pardos, D. Domínguez Damiani, G. Eckerlin, T. Eichhorn, A. Elwood, E. Eren, E. Gallo[17], A. Geiser, J.M. Grados Luyando, A. Grohsjean, M. Guthoff, M. Haranko, A. Harb, J. Hauk, H. Jung, M. Kasemann, J. Keaveney, C. Kleinwort, J. Knolle, D. Krücker, W. Lange, A. Lelek, T. Lenz, J. Leonard, K. Lipka, W. Lohmann[18], R. Mankel, I.-A. Melzer-Pellmann, A.B. Meyer, M. Meyer, M. Missiroli, G. Mittag, J. Mnich, V. Myronenko, S.K. Pflitsch, D. Pitzl, A. Raspereza, M. Savitskyi, P. Saxena, P. Schütze, C. Schwanenberger, R. Shevchenko, A. Singh, H. Tholen, O. Turkot, A. Vagnerini, G.P. Van Onsem, R. Walsh, Y. Wen, K. Wichmann, C. Wissing, O. Zenaiev

University of Hamburg, Hamburg, Germany
R. Aggleton, S. Bein, L. Benato, A. Benecke, V. Blobel, T. Dreyer, A. Ebrahimi, E. Garutti, D. Gonzalez, P. Gunnellini, J. Haller, A. Hinzmann, A. Karavdina, G. Kasieczka, R. Klanner, R. Kogler, N. Kovalchuk, S. Kurz, V. Kutzner, J. Lange, D. Marconi, J. Multhaup, M. Niedziela, C.E.N. Niemeyer, D. Nowatschin, A. Perieanu, A. Reimers, O. Rieger, C. Scharf, P. Schleper, S. Schumann, J. Schwandt, J. Sonneveld, H. Stadie, G. Steinbrück, F.M. Stober, M. Stöver, A. Vanhoefer, B. Vormwald, I. Zoi

Karlsruher Institut fuer Technologie, Karlsruhe, Germany
M. Akbiyik, C. Barth, M. Baselga, S. Baur, E. Butz, R. Caspart, T. Chwalek, F. Colombo, W. De Boer, A. Dierlamm, K. El Morabit, N. Faltermann, B. Freund, M. Giffels, M.A. Harrendorf, F. Hartmann[15], S.M. Heindl, U. Husemann, I. Katkov[14], S. Kudella, S. Mitra, M.U. Mozer, Th. Müller, M. Musich, M. Plagge, G. Quast, K. Rabbertz, M. Schröder, I. Shvetsov, H.J. Simonis, R. Ulrich, S. Wayand, M. Weber, T. Weiler, C. Wöhrmann, R. Wolf

Institute of Nuclear and Particle Physics (INPP), NCSR Demokritos, Aghia Paraskevi, Greece
G. Anagnostou, G. Daskalakis, T. Geralis, A. Kyriakis, D. Loukas, G. Paspalaki

National and Kapodistrian University of Athens, Athens, Greece
G. Karathanasis, P. Kontaxakis, A. Panagiotou, I. Papavergou, N. Saoulidou, E. Tziaferi, K. Vellidis

National Technical University of Athens, Athens, Greece
K. Kousouris, I. Papakrivopoulos, G. Tsipolitis

University of Ioánnina, Ioánnina, Greece
I. Evangelou, C. Foudas, P. Gianneios, P. Katsoulis, P. Kokkas, S. Mallios, N. Manthos, I. Papadopoulos, E. Paradas, J. Strologas, F.A. Triantis, D. Tsitsonis

MTA-ELTE Lendület CMS Particle and Nuclear Physics Group, Eötvös Loránd University, Budapest, Hungary
M. Bartók[19], M. Csanad, N. Filipovic, P. Major, M.I. Nagy, G. Pasztor, O. Surányi, G.I. Veres

Wigner Research Centre for Physics, Budapest, Hungary
G. Bencze, C. Hajdu, D. Horvath[20], Á. Hunyadi, F. Sikler, T.Á. Vámi, V. Veszpremi, G. Vesztergombi†

Institute of Nuclear Research ATOMKI, Debrecen, Hungary
N. Beni, S. Czellar, J. Karancsi[19], A. Makovec, J. Molnar, Z. Szillasi

Institute of Physics, University of Debrecen, Debrecen, Hungary
P. Raics, Z.L. Trocsanyi, B. Ujvari

Indian Institute of Science (IISc), Bangalore, India
S. Choudhury, J.R. Komaragiri, P.C. Tiwari

National Institute of Science Education and Research, HBNI, Bhubaneswar, India
S. Bahinipati[22], C. Kar, P. Mal, K. Mandal, A. Nayak[23], D.K. Sahoo[22], S.K. Swain

Panjab University, Chandigarh, India
S. Bansal, S.B. Beri, V. Bhatnagar, S. Chauhan, R. Chawla, N. Dhingra, R. Gupta, A. Kaur, M. Kaur, S. Kaur, P. Kumari, M. Lohan, A. Mehta, K. Sandeep, S. Sharma, J.B. Singh, A.K. Virdi, G. Walia

University of Delhi, Delhi, India
A. Bhardwaj, B.C. Choudhary, R.B. Garg, M. Gola, S. Keshri, Ashok Kumar, S. Malhotra, M. Naimuddin, P. Priyanka, K. Ranjan, Aashaq Shah, R. Sharma

Saha Institute of Nuclear Physics, HBNI, Kolkata, India
R. Bhardwaj[24], M. Bharti[24], R. Bhattacharya, S. Bhattacharya, U. Bhawandeep[24], D. Bhowmik, S. Dey, S. Dutt[24], S. Dutta, S. Ghosh, K. Mondal, S. Nandan, A. Purohit, P.K. Rout, A. Roy, S. Roy Chowdhury, G. Saha, S. Sarkar, M. Sharan, B. Singh[24], S. Thakur[24]

Indian Institute of Technology Madras, Madras, India
P.K. Behera

Bhabha Atomic Research Centre, Mumbai, India
R. Chudasama, D. Dutta, V. Jha, V. Kumar, P.K. Netrakanti, L.M. Pant, P. Shukla

Tata Institute of Fundamental Research-A, Mumbai, India
T. Aziz, M.A. Bhat, S. Dugad, G.B. Mohanty, N. Sur, B. Sutar, RavindraKumar Verma

Tata Institute of Fundamental Research-B, Mumbai, India
S. Banerjee, S. Bhattacharya, S. Chatterjee, P. Das, M. Guchait, Sa. Jain, S. Karmakar, S. Kumar, M. Maity[25], G. Majumder, K. Mazumdar, N. Sahoo, T. Sarkar[25]

Indian Institute of Science Education and Research (IISER), Pune, India
S. Chauhan, S. Dube, V. Hegde, A. Kapoor, K. Kothekar, S. Pandey, A. Rane, A. Rastogi, S. Sharma

Institute for Research in Fundamental Sciences (IPM), Tehran, Iran
S. Chenarani[26], E. Eskandari Tadavani, S.M. Etesami[26], M. Khakzad, M. Mohammadi Najafabadi, M. Naseri, F. Rezaei Hosseinabadi, B. Safarzadeh[27], M. Zeinali

University College Dublin, Dublin, Ireland
M. Felcini, M. Grunewald

INFN Sezione di Bari [a], Università di Bari [b], Politecnico di Bari [c], Bari, Italy
M. Abbrescia[a,b], C. Calabria[a,b], A. Colaleo[a], D. Creanza[a,c], L. Cristella[a,b], N. De Filippis[a,c], M. De Palma[a,b], A. Di Florio[a,b], F. Errico[a,b], L. Fiore[a], A. Gelmi[a,b], G. Iaselli[a,c], M. Ince[a,b], S. Lezki[a,b], G. Maggi[a,c], M. Maggi[a], G. Miniello[a,b], S. My[a,b], S. Nuzzo[a,b], A. Pompili[a,b], G. Pugliese[a,c], R. Radogna[a], A. Ranieri[a], G. Selvaggi[a,b], A. Sharma[a], L. Silvestris[a], R. Venditti[a], P. Verwilligen[a], G. Zito[a]

INFN Sezione di Bologna [a], Università di Bologna [b], Bologna, Italy
G. Abbiendi[a], C. Battilana[a,b], D. Bonacorsi[a,b], L. Borgonovi[a,b], S. Braibant-Giacomelli[a,b], R. Campanini[a,b], P. Capiluppi[a,b], A. Castro[a,b], F.R. Cavallo[a], S.S. Chhibra[a,b], C. Ciocca[a], G. Codispoti[a,b], M. Cuffiani[a,b], G.M. Dallavalle[a], F. Fabbri[a], A. Fanfani[a,b], E. Fontanesi, P. Giacomelli[a], C. Grandi[a], L. Guiducci[a,b], F. Iemmi[a,b], S. Lo Meo[a], S. Marcellini[a], G. Masetti[a], A. Montanari[a], F.L. Navarria[a,b], A. Perrotta[a], F. Primavera[a,b,15], T. Rovelli[a,b], G.P. Siroli[a,b], N. Tosi[a]

INFN Sezione di Catania [a], Università di Catania [b], Catania, Italy
S. Albergo[a,b], A. Di Mattia[a], R. Potenza[a,b], A. Tricomi[a,b], C. Tuve[a,b]

INFN Sezione di Firenze [a], Università di Firenze [b], Firenze, Italy
G. Barbagli[a], K. Chatterjee[a,b], V. Ciulli[a,b], C. Civinini[a], R. D'Alessandro[a,b], E. Focardi[a,b], G. Latino, P. Lenzi[a,b], M. Meschini[a], S. Paoletti[a], L. Russo[a,28], G. Sguazzoni[a], D. Strom[a], L. Viliani[a]

INFN Laboratori Nazionali di Frascati, Frascati, Italy
L. Benussi, S. Bianco, F. Fabbri, D. Piccolo

INFN Sezione di Genova [a], Università di Genova [b], Genova, Italy
F. Ferro[a], R. Mulargia[a,b], F. Ravera[a,b], E. Robutti[a], S. Tosi[a,b]

INFN Sezione di Milano-Bicocca [a], Università di Milano-Bicocca [b], Milano, Italy
A. Benaglia[a], A. Beschi[b], F. Brivio[a,b], V. Ciriolo[a,b,15], S. Di Guida[a,d,15], M.E. Dinardo[a,b], S. Fiorendi[a,b], S. Gennai[a], A. Ghezzi[a,b], P. Govoni[a,b], M. Malberti[a,b], S. Malvezzi[a], A. Massironi[a,b], D. Menasce[a], F. Monti, L. Moroni[a], M. Paganoni[a,b], D. Pedrini[a], S. Ragazzi[a,b], T. Tabarelli de Fatis[a,b], D. Zuolo[a,b]

INFN Sezione di Napoli [a], Università di Napoli 'Federico II' [b], Napoli, Italy, Università della Basilicata [c], Potenza, Italy, Università G. Marconi [d], Roma, Italy
S. Buontempo[a], N. Cavallo[a,c], A. De Iorio[a,b], A. Di Crescenzo[a,b], F. Fabozzi[a,c], F. Fienga[a], G. Galati[a], A.O.M. Iorio[a,b], W.A. Khan[a], L. Lista[a], S. Meola[a,d,15], P. Paolucci[a,15], C. Sciacca[a,b], E. Voevodina[a,b]

INFN Sezione di Padova [a], Università di Padova [b], Padova, Italy, Università di Trento [c], Trento, Italy
P. Azzi[a], N. Bacchetta[a], D. Bisello[a,b], A. Boletti[a,b], A. Bragagnolo, R. Carlin[a,b], P. Checchia[a], M. Dall'Osso[a,b], P. De Castro Manzano[a], T. Dorigo[a], U. Dosselli[a], U. Gasparini[a,b], A. Gozzelino[a], S.Y. Hoh, S. Lacaprara[a], P. Lujan, M. Margoni[a,b], A.T. Meneguzzo[a,b], J. Pazzini[a,b], N. Pozzobon[a,b], P. Ronchese[a,b], R. Rossin[a,b], F. Simonetto[a,b], A. Tiko, E. Torassa[a], M. Tosi[a,b], M. Zanetti[a,b], P. Zotto[a,b], G. Zumerle[a,b]

INFN Sezione di Pavia [a], Università di Pavia [b], Pavia, Italy
A. Braghieri[a], A. Magnani[a], P. Montagna[a,b], S.P. Ratti[a,b], V. Re[a], M. Ressegotti[a,b], C. Riccardi[a,b], P. Salvini[a], I. Vai[a,b], P. Vitulo[a,b]

INFN Sezione di Perugia [a], Università di Perugia [b], Perugia, Italy
M. Biasini[a,b], G.M. Bilei[a], C. Cecchi[a,b], D. Ciangottini[a,b], L. Fanò[a,b], P. Lariccia[a,b], R. Leonardi[a,b], E. Manoni[a], G. Mantovani[a,b], V. Mariani[a,b], M. Menichelli[a], A. Rossi[a,b], A. Santocchia[a,b], D. Spiga[a]

INFN Sezione di Pisa [a], Università di Pisa [b], Scuola Normale Superiore di Pisa [c], Pisa, Italy
K. Androsov[a], P. Azzurri[a], G. Bagliesi[a], L. Bianchini[a], T. Boccali[a], L. Borrello, R. Castaldi[a], M.A. Ciocci[a,b], R. Dell'Orso[a], G. Fedi[a], F. Fiori[a,c], L. Giannini[a,c], A. Giassi[a], M.T. Grippo[a],

F. Ligabue[a,c], E. Manca[a,c], G. Mandorli[a,c], A. Messineo[a,b], F. Palla[a], A. Rizzi[a,b], G. Rolandi[29], P. Spagnolo[a], R. Tenchini[a], G. Tonelli[a,b], A. Venturi[a], P.G. Verdini[a]

INFN Sezione di Roma [a], Sapienza Università di Roma [b], Rome, Italy
L. Barone[a,b], F. Cavallari[a], M. Cipriani[a,b], D. Del Re[a,b], E. Di Marco[a,b], M. Diemoz[a], S. Gelli[a,b], E. Longo[a,b], B. Marzocchi[a,b], P. Meridiani[a], G. Organtini[a,b], F. Pandolfi[a], R. Paramatti[a,b], F. Preiato[a,b], S. Rahatlou[a,b], C. Rovelli[a], F. Santanastasio[a,b]

INFN Sezione di Torino [a], Università di Torino [b], Torino, Italy, Università del Piemonte Orientale [c], Novara, Italy
N. Amapane[a,b], R. Arcidiacono[a,c], S. Argiro[a,b], M. Arneodo[a,c], N. Bartosik[a], R. Bellan[a,b], C. Biino[a], A. Cappati[a,b], N. Cartiglia[a], F. Cenna[a,b], S. Cometti[a], M. Costa[a,b], R. Covarelli[a,b], N. Demaria[a], B. Kiani[a,b], C. Mariotti[a], S. Maselli[a], E. Migliore[a,b], V. Monaco[a,b], E. Monteil[a,b], M. Monteno[a], M.M. Obertino[a,b], L. Pacher[a,b], N. Pastrone[a], M. Pelliccioni[a], G.L. Pinna Angioni[a,b], A. Romero[a,b], M. Ruspa[a,c], R. Sacchi[a,b], R. Salvatico[a,b], K. Shchelina[a,b], V. Sola[a], A. Solano[a,b], D. Soldi[a,b], A. Staiano[a]

INFN Sezione di Trieste [a], Università di Trieste [b], Trieste, Italy
S. Belforte[a], V. Candelise[a,b], M. Casarsa[a], F. Cossutti[a], A. Da Rold[a,b], G. Della Ricca[a,b], F. Vazzoler[a,b], A. Zanetti[a]

Kyungpook National University, Daegu, Korea
D.H. Kim, G.N. Kim, M.S. Kim, J. Lee, S. Lee, S.W. Lee, C.S. Moon, Y.D. Oh, S.I. Pak, S. Sekmen, D.C. Son, Y.C. Yang

Chonnam National University, Institute for Universe and Elementary Particles, Kwangju, Korea
H. Kim, D.H. Moon, G. Oh

Hanyang University, Seoul, Korea
B. Francois, J. Goh[30], T.J. Kim

Korea University, Seoul, Korea
S. Cho, S. Choi, Y. Go, D. Gyun, S. Ha, B. Hong, Y. Jo, K. Lee, K.S. Lee, S. Lee, J. Lim, S.K. Park, Y. Roh

Sejong University, Seoul, Korea
H.S. Kim

Seoul National University, Seoul, Korea
J. Almond, J. Kim, J.S. Kim, H. Lee, K. Lee, K. Nam, S.B. Oh, B.C. Radburn-Smith, S.h. Seo, U.K. Yang, H.D. Yoo, G.B. Yu

University of Seoul, Seoul, Korea
D. Jeon, H. Kim, J.H. Kim, J.S.H. Lee, I.C. Park

Sungkyunkwan University, Suwon, Korea
Y. Choi, C. Hwang, J. Lee, I. Yu

Vilnius University, Vilnius, Lithuania
V. Dudenas, A. Juodagalvis, J. Vaitkus

National Centre for Particle Physics, Universiti Malaya, Kuala Lumpur, Malaysia
I. Ahmed, Z.A. Ibrahim, M.A.B. Md Ali[31], F. Mohamad Idris[32], W.A.T. Wan Abdullah, M.N. Yusli, Z. Zolkapli

Universidad de Sonora (UNISON), Hermosillo, Mexico
J.F. Benitez, A. Castaneda Hernandez, J.A. Murillo Quijada

Centro de Investigacion y de Estudios Avanzados del IPN, Mexico City, Mexico
H. Castilla-Valdez, E. De La Cruz-Burelo, M.C. Duran-Osuna, I. Heredia-De La Cruz[33], R. Lopez-Fernandez, J. Mejia Guisao, R.I. Rabadan-Trejo, M. Ramirez-Garcia, G. Ramirez-Sanchez, R. Reyes-Almanza, A. Sanchez-Hernandez

Universidad Iberoamericana, Mexico City, Mexico
S. Carrillo Moreno, C. Oropeza Barrera, F. Vazquez Valencia

Benemerita Universidad Autonoma de Puebla, Puebla, Mexico
J. Eysermans, I. Pedraza, H.A. Salazar Ibarguen, C. Uribe Estrada

Universidad Autónoma de San Luis Potosí, San Luis Potosí, Mexico
A. Morelos Pineda

University of Auckland, Auckland, New Zealand
D. Krofcheck

University of Canterbury, Christchurch, New Zealand
S. Bheesette, P.H. Butler

National Centre for Physics, Quaid-I-Azam University, Islamabad, Pakistan
A. Ahmad, M. Ahmad, M.I. Asghar, Q. Hassan, H.R. Hoorani, A. Saddique, M.A. Shah, M. Shoaib, M. Waqas

National Centre for Nuclear Research, Swierk, Poland
H. Bialkowska, M. Bluj, B. Boimska, T. Frueboes, M. Górski, M. Kazana, M. Szleper, P. Traczyk, P. Zalewski

Institute of Experimental Physics, Faculty of Physics, University of Warsaw, Warsaw, Poland
K. Bunkowski, A. Byszuk[34], K. Doroba, A. Kalinowski, M. Konecki, J. Krolikowski, M. Misiura, M. Olszewski, A. Pyskir, M. Walczak

Laboratório de Instrumentação e Física Experimental de Partículas, Lisboa, Portugal
M. Araujo, P. Bargassa, C. Beirão Da Cruz E Silva, A. Di Francesco, P. Faccioli, B. Galinhas, M. Gallinaro, J. Hollar, N. Leonardo, J. Seixas, G. Strong, O. Toldaiev, J. Varela

Joint Institute for Nuclear Research, Dubna, Russia
S. Afanasiev, P. Bunin, M. Gavrilenko, I. Golutvin, I. Gorbunov, A. Kamenev, V. Karjavine, A. Lanev, A. Malakhov, V. Matveev[35,36], P. Moisenz, V. Palichik, V. Perelygin, S. Shmatov, S. Shulha, N. Skatchkov, V. Smirnov, N. Voytishin, A. Zarubin

Petersburg Nuclear Physics Institute, Gatchina (St. Petersburg), Russia
V. Golovtsov, Y. Ivanov, V. Kim[37], E. Kuznetsova[38], P. Levchenko, V. Murzin, V. Oreshkin, I. Smirnov, D. Sosnov, V. Sulimov, L. Uvarov, S. Vavilov, A. Vorobyev

Institute for Nuclear Research, Moscow, Russia
Yu. Andreev, A. Dermenev, S. Gninenko, N. Golubev, A. Karneyeu, M. Kirsanov, N. Krasnikov, A. Pashenkov, D. Tlisov, A. Toropin

Institute for Theoretical and Experimental Physics, Moscow, Russia
V. Epshteyn, V. Gavrilov, N. Lychkovskaya, V. Popov, I. Pozdnyakov, G. Safronov, A. Spiridonov, A. Stepennov, V. Stolin, M. Toms, E. Vlasov, A. Zhokin

Moscow Institute of Physics and Technology, Moscow, Russia
T. Aushev

National Research Nuclear University 'Moscow Engineering Physics Institute' (MEPhI), Moscow, Russia
R. Chistov[39], M. Danilov[39], P. Parygin, D. Philippov, S. Polikarpov[39], E. Tarkovskii

P.N. Lebedev Physical Institute, Moscow, Russia
V. Andreev, M. Azarkin, I. Dremin[36], M. Kirakosyan, A. Terkulov

Skobeltsyn Institute of Nuclear Physics, Lomonosov Moscow State University, Moscow, Russia
A. Baskakov, A. Belyaev, E. Boos, M. Dubinin[40], L. Dudko, A. Ershov, A. Gribushin, V. Klyukhin, O. Kodolova, I. Lokhtin, I. Miagkov, S. Obraztsov, S. Petrushanko, V. Savrin, A. Snigirev

Novosibirsk State University (NSU), Novosibirsk, Russia
A. Barnyakov[41], V. Blinov[41], T. Dimova[41], L. Kardapoltsev[41], Y. Skovpen[41]

Institute for High Energy Physics of National Research Centre 'Kurchatov Institute', Protvino, Russia
I. Azhgirey, I. Bayshev, S. Bitioukov, D. Elumakhov, A. Godizov, V. Kachanov, A. Kalinin, D. Konstantinov, P. Mandrik, V. Petrov, R. Ryutin, S. Slabospitskii, A. Sobol, S. Troshin, N. Tyurin, A. Uzunian, A. Volkov

National Research Tomsk Polytechnic University, Tomsk, Russia
A. Babaev, S. Baidali, V. Okhotnikov

University of Belgrade, Faculty of Physics and Vinca Institute of Nuclear Sciences, Belgrade, Serbia
P. Adzic[42], P. Cirkovic, D. Devetak, M. Dordevic, J. Milosevic

Centro de Investigaciones Energéticas Medioambientales y Tecnológicas (CIEMAT), Madrid, Spain
J. Alcaraz Maestre, A. Álvarez Fernández, I. Bachiller, M. Barrio Luna, J.A. Brochero Cifuentes, M. Cerrada, N. Colino, B. De La Cruz, A. Delgado Peris, C. Fernandez Bedoya, J.P. Fernández Ramos, J. Flix, M.C. Fouz, O. Gonzalez Lopez, S. Goy Lopez, J.M. Hernandez, M.I. Josa, D. Moran, A. Pérez-Calero Yzquierdo, J. Puerta Pelayo, I. Redondo, L. Romero, M.S. Soares, A. Triossi

Universidad Autónoma de Madrid, Madrid, Spain
C. Albajar, J.F. de Trocóniz

Universidad de Oviedo, Oviedo, Spain
J. Cuevas, C. Erice, J. Fernandez Menendez, S. Folgueras, I. Gonzalez Caballero, J.R. González Fernández, E. Palencia Cortezon, V. Rodríguez Bouza, S. Sanchez Cruz, P. Vischia, J.M. Vizan Garcia

Instituto de Física de Cantabria (IFCA), CSIC-Universidad de Cantabria, Santander, Spain
I.J. Cabrillo, A. Calderon, B. Chazin Quero, J. Duarte Campderros, M. Fernandez, P.J. Fernández Manteca, A. García Alonso, J. Garcia-Ferrero, G. Gomez, A. Lopez Virto, J. Marco, C. Martinez Rivero, P. Martinez Ruiz del Arbol, F. Matorras, J. Piedra Gomez, C. Prieels, T. Rodrigo, A. Ruiz-Jimeno, L. Scodellaro, N. Trevisani, I. Vila, R. Vilar Cortabitarte

University of Ruhuna, Department of Physics, Matara, Sri Lanka
N. Wickramage

CERN, European Organization for Nuclear Research, Geneva, Switzerland
D. Abbaneo, B. Akgun, E. Auffray, G. Auzinger, P. Baillon, A.H. Ball, D. Barney, J. Bendavid, M. Bianco, A. Bocci, C. Botta, E. Brondolin, T. Camporesi, M. Cepeda, G. Cerminara, E. Chapon, Y. Chen, G. Cucciati, D. d'Enterria, A. Dabrowski, N. Daci, V. Daponte, A. David, A. De Roeck, N. Deelen, M. Dobson, M. Dünser, N. Dupont, A. Elliott-Peisert, P. Everaerts, F. Fallavollita[43], D. Fasanella, G. Franzoni, J. Fulcher, W. Funk, D. Gigi, A. Gilbert, K. Gill, F. Glege, M. Gruchala, M. Guilbaud, D. Gulhan, J. Hegeman, C. Heidegger, V. Innocente, A. Jafari, P. Janot, O. Karacheban[18], J. Kieseler, A. Kornmayer, M. Krammer[1], C. Lange, P. Lecoq, C. Lourenço, L. Malgeri, M. Mannelli, F. Meijers, J.A. Merlin, S. Mersi, E. Meschi, P. Milenovic[44], F. Moortgat, M. Mulders, J. Ngadiuba, S. Nourbakhsh, S. Orfanelli, L. Orsini, F. Pantaleo[15], L. Pape, E. Perez, M. Peruzzi, A. Petrilli, G. Petrucciani, A. Pfeiffer, M. Pierini, F.M. Pitters, D. Rabady, A. Racz, T. Reis, M. Rovere, H. Sakulin, C. Schäfer, C. Schwick, M. Seidel, M. Selvaggi, A. Sharma, P. Silva, P. Sphicas[45], A. Stakia, J. Steggemann, D. Treille, A. Tsirou, V. Veckalns[46], M. Verzetti, W.D. Zeuner

Paul Scherrer Institut, Villigen, Switzerland
L. Caminada[47], K. Deiters, W. Erdmann, R. Horisberger, Q. Ingram, H.C. Kaestli, D. Kotlinski, U. Langenegger, T. Rohe, S.A. Wiederkehr

ETH Zurich - Institute for Particle Physics and Astrophysics (IPA), Zurich, Switzerland
M. Backhaus, L. Bäni, P. Berger, N. Chernyavskaya, G. Dissertori, M. Dittmar, M. Donegà, C. Dorfer, T.A. Gómez Espinosa, C. Grab, D. Hits, T. Klijnsma, W. Lustermann, R.A. Manzoni, M. Marionneau, M.T. Meinhard, F. Micheli, P. Musella, F. Nessi-Tedaldi, J. Pata, F. Pauss, G. Perrin, L. Perrozzi, S. Pigazzini, M. Quittnat, C. Reissel, D. Ruini, D.A. Sanz Becerra, M. Schönenberger, L. Shchutska, V.R. Tavolaro, K. Theofilatos, M.L. Vesterbacka Olsson, R. Wallny, D.H. Zhu

Universität Zürich, Zurich, Switzerland
T.K. Aarrestad, C. Amsler[48], D. Brzhechko, M.F. Canelli, A. De Cosa, R. Del Burgo, S. Donato, C. Galloni, T. Hreus, B. Kilminster, S. Leontsinis, I. Neutelings, G. Rauco, P. Robmann, D. Salerno, K. Schweiger, C. Seitz, Y. Takahashi, A. Zucchetta

National Central University, Chung-Li, Taiwan
T.H. Doan, R. Khurana, C.M. Kuo, W. Lin, A. Pozdnyakov, S.S. Yu

National Taiwan University (NTU), Taipei, Taiwan
P. Chang, Y. Chao, K.F. Chen, P.H. Chen, W.-S. Hou, Arun Kumar, Y.F. Liu, R.-S. Lu, E. Paganis, A. Psallidas, A. Steen

Chulalongkorn University, Faculty of Science, Department of Physics, Bangkok, Thailand
B. Asavapibhop, N. Srimanobhas, N. Suwonjandee

Çukurova University, Physics Department, Science and Art Faculty, Adana, Turkey
A. Bat, F. Boran, S. Damarseckin, Z.S. Demiroglu, F. Dolek, C. Dozen, I. Dumanoglu, S. Girgis, G. Gokbulut, Y. Guler, E. Gurpinar, I. Hos[49], C. Isik, E.E. Kangal[50], O. Kara, A. Kayis Topaksu, U. Kiminsu, M. Oglakci, G. Onengut, K. Ozdemir[51], S. Ozturk[52], D. Sunar Cerci[53], B. Tali[53], U.G. Tok, H. Topakli[52], S. Turkcapar, I.S. Zorbakir, C. Zorbilmez

Middle East Technical University, Physics Department, Ankara, Turkey
B. Isildak[54], G. Karapinar[55], M. Yalvac, M. Zeyrek

Bogazici University, Istanbul, Turkey
I.O. Atakisi, E. Gülmez, M. Kaya[56], O. Kaya[57], S. Ozkorucuklu[58], S. Tekten, E.A. Yetkin[59]

Istanbul Technical University, Istanbul, Turkey
M.N. Agaras, A. Cakir, K. Cankocak, Y. Komurcu, S. Sen[60]

Institute for Scintillation Materials of National Academy of Science of Ukraine, Kharkov, Ukraine
B. Grynyov

National Scientific Center, Kharkov Institute of Physics and Technology, Kharkov, Ukraine
L. Levchuk

University of Bristol, Bristol, United Kingdom
F. Ball, J.J. Brooke, D. Burns, E. Clement, D. Cussans, O. Davignon, H. Flacher, J. Goldstein, G.P. Heath, H.F. Heath, L. Kreczko, D.M. Newbold[61], S. Paramesvaran, B. Penning, T. Sakuma, D. Smith, V.J. Smith, J. Taylor, A. Titterton

Rutherford Appleton Laboratory, Didcot, United Kingdom
K.W. Bell, A. Belyaev[62], C. Brew, R.M. Brown, D. Cieri, D.J.A. Cockerill, J.A. Coughlan, K. Harder, S. Harper, J. Linacre, E. Olaiya, D. Petyt, C.H. Shepherd-Themistocleous, A. Thea, I.R. Tomalin, T. Williams, W.J. Womersley

Imperial College, London, United Kingdom
R. Bainbridge, P. Bloch, J. Borg, S. Breeze, O. Buchmuller, A. Bundock, D. Colling, P. Dauncey, G. Davies, M. Della Negra, R. Di Maria, G. Hall, G. Iles, T. James, M. Komm, C. Laner, L. Lyons, A.-M. Magnan, S. Malik, A. Martelli, J. Nash[63], A. Nikitenko[7], V. Palladino, M. Pesaresi, D.M. Raymond, A. Richards, A. Rose, E. Scott, C. Seez, A. Shtipliyski, G. Singh, M. Stoye, T. Strebler, S. Summers, A. Tapper, K. Uchida, T. Virdee[15], N. Wardle, D. Winterbottom, J. Wright, S.C. Zenz

Brunel University, Uxbridge, United Kingdom
J.E. Cole, P.R. Hobson, A. Khan, P. Kyberd, C.K. Mackay, A. Morton, I.D. Reid, L. Teodorescu, S. Zahid

Baylor University, Waco, USA
K. Call, J. Dittmann, K. Hatakeyama, H. Liu, C. Madrid, B. McMaster, N. Pastika, C. Smith

Catholic University of America, Washington, DC, USA
R. Bartek, A. Dominguez

The University of Alabama, Tuscaloosa, USA
A. Buccilli, S.I. Cooper, C. Henderson, P. Rumerio, C. West

Boston University, Boston, USA
D. Arcaro, T. Bose, D. Gastler, D. Pinna, D. Rankin, C. Richardson, J. Rohlf, L. Sulak, D. Zou

Brown University, Providence, USA
G. Benelli, X. Coubez, D. Cutts, M. Hadley, J. Hakala, U. Heintz, J.M. Hogan[64], K.H.M. Kwok, E. Laird, G. Landsberg, J. Lee, Z. Mao, M. Narain, S. Sagir[65], R. Syarif, E. Usai, D. Yu

University of California, Davis, Davis, USA
R. Band, C. Brainerd, R. Breedon, D. Burns, M. Calderon De La Barca Sanchez, M. Chertok, J. Conway, R. Conway, P.T. Cox, R. Erbacher, C. Flores, G. Funk, W. Ko, O. Kukral, R. Lander, M. Mulhearn, D. Pellett, J. Pilot, S. Shalhout, M. Shi, D. Stolp, D. Taylor, K. Tos, M. Tripathi, Z. Wang, F. Zhang

University of California, Los Angeles, USA
M. Bachtis, C. Bravo, R. Cousins, A. Dasgupta, A. Florent, J. Hauser, M. Ignatenko, N. Mccoll, S. Regnard, D. Saltzberg, C. Schnaible, V. Valuev

University of California, Riverside, Riverside, USA
E. Bouvier, K. Burt, R. Clare, J.W. Gary, S.M.A. Ghiasi Shirazi, G. Hanson, G. Karapostoli, E. Kennedy, F. Lacroix, O.R. Long, M. Olmedo Negrete, M.I. Paneva, W. Si, L. Wang, H. Wei, S. Wimpenny, B.R. Yates

University of California, San Diego, La Jolla, USA
J.G. Branson, P. Chang, S. Cittolin, M. Derdzinski, R. Gerosa, D. Gilbert, B. Hashemi, A. Holzner, D. Klein, G. Kole, V. Krutelyov, J. Letts, M. Masciovecchio, D. Olivito, S. Padhi, M. Pieri, M. Sani, V. Sharma, S. Simon, M. Tadel, A. Vartak, S. Wasserbaech[66], J. Wood, F. Würthwein, A. Yagil, G. Zevi Della Porta

University of California, Santa Barbara - Department of Physics, Santa Barbara, USA
N. Amin, R. Bhandari, C. Campagnari, M. Citron, V. Dutta, M. Franco Sevilla, L. Gouskos, R. Heller, J. Incandela, A. Ovcharova, H. Qu, J. Richman, D. Stuart, I. Suarez, S. Wang, J. Yoo

California Institute of Technology, Pasadena, USA
D. Anderson, A. Bornheim, J.M. Lawhorn, N. Lu, H.B. Newman, T.Q. Nguyen, M. Spiropulu, J.R. Vlimant, R. Wilkinson, S. Xie, Z. Zhang, R.Y. Zhu

Carnegie Mellon University, Pittsburgh, USA
M.B. Andrews, T. Ferguson, T. Mudholkar, M. Paulini, M. Sun, I. Vorobiev, M. Weinberg

University of Colorado Boulder, Boulder, USA
J.P. Cumalat, W.T. Ford, F. Jensen, A. Johnson, E. MacDonald, T. Mulholland, R. Patel, A. Perloff, K. Stenson, K.A. Ulmer, S.R. Wagner

Cornell University, Ithaca, USA
J. Alexander, J. Chaves, Y. Cheng, J. Chu, A. Datta, K. Mcdermott, N. Mirman, J.R. Patterson, D. Quach, A. Rinkevicius, A. Ryd, L. Skinnari, L. Soffi, S.M. Tan, Z. Tao, J. Thom, J. Tucker, P. Wittich, M. Zientek

Fermi National Accelerator Laboratory, Batavia, USA
S. Abdullin, M. Albrow, M. Alyari, G. Apollinari, A. Apresyan, A. Apyan, S. Banerjee, L.A.T. Bauerdick, A. Beretvas, J. Berryhill, P.C. Bhat, K. Burkett, J.N. Butler, A. Canepa, G.B. Cerati, H.W.K. Cheung, F. Chlebana, M. Cremonesi, J. Duarte, V.D. Elvira, J. Freeman, Z. Gecse, E. Gottschalk, L. Gray, D. Green, S. Grünendahl, O. Gutsche, J. Hanlon, R.M. Harris, S. Hasegawa, J. Hirschauer, Z. Hu, B. Jayatilaka, S. Jindariani, M. Johnson, U. Joshi, B. Klima, M.J. Kortelainen, B. Kreis, S. Lammel, D. Lincoln, R. Lipton, M. Liu, T. Liu, J. Lykken, K. Maeshima, J.M. Marraffino, D. Mason, P. McBride, P. Merkel, S. Mrenna, S. Nahn, V. O'Dell, K. Pedro, C. Pena, O. Prokofyev, G. Rakness, L. Ristori, A. Savoy-Navarro[67], B. Schneider, E. Sexton-Kennedy, A. Soha, W.J. Spalding, L. Spiegel, S. Stoynev, J. Strait, N. Strobbe, L. Taylor, S. Tkaczyk, N.V. Tran, L. Uplegger, E.W. Vaandering, C. Vernieri, M. Verzocchi, R. Vidal, M. Wang, H.A. Weber, A. Whitbeck

University of Florida, Gainesville, USA
D. Acosta, P. Avery, P. Bortignon, D. Bourilkov, A. Brinkerhoff, L. Cadamuro, A. Carnes, D. Curry, R.D. Field, S.V. Gleyzer, B.M. Joshi, J. Konigsberg, A. Korytov, K.H. Lo, P. Ma, K. Matchev, H. Mei, G. Mitselmakher, D. Rosenzweig, K. Shi, D. Sperka, J. Wang, S. Wang, X. Zuo

Florida International University, Miami, USA
Y.R. Joshi, S. Linn

Florida State University, Tallahassee, USA
A. Ackert, T. Adams, A. Askew, S. Hagopian, V. Hagopian, K.F. Johnson, T. Kolberg, G. Martinez, T. Perry, H. Prosper, A. Saha, C. Schiber, R. Yohay

Florida Institute of Technology, Melbourne, USA
M.M. Baarmand, V. Bhopatkar, S. Colafranceschi, M. Hohlmann, D. Noonan, M. Rahmani, T. Roy, F. Yumiceva

University of Illinois at Chicago (UIC), Chicago, USA
M.R. Adams, L. Apanasevich, D. Berry, R.R. Betts, R. Cavanaugh, X. Chen, S. Dittmer, O. Evdokimov, C.E. Gerber, D.A. Hangal, D.J. Hofman, K. Jung, J. Kamin, C. Mills, I.D. Sandoval Gonzalez, M.B. Tonjes, H. Trauger, N. Varelas, H. Wang, X. Wang, Z. Wu, J. Zhang

The University of Iowa, Iowa City, USA
M. Alhusseini, B. Bilki[68], W. Clarida, K. Dilsiz[69], S. Durgut, R.P. Gandrajula, M. Haytmyradov, V. Khristenko, J.-P. Merlo, A. Mestvirishvili, A. Moeller, J. Nachtman, H. Ogul[70], Y. Onel, F. Ozok[71], A. Penzo, C. Snyder, E. Tiras, J. Wetzel

Johns Hopkins University, Baltimore, USA
B. Blumenfeld, A. Cocoros, N. Eminizer, D. Fehling, L. Feng, A.V. Gritsan, W.T. Hung, P. Maksimovic, J. Roskes, U. Sarica, M. Swartz, M. Xiao, C. You

The University of Kansas, Lawrence, USA
A. Al-bataineh, P. Baringer, A. Bean, S. Boren, J. Bowen, A. Bylinkin, J. Castle, S. Khalil, A. Kropivnitskaya, D. Majumder, W. Mcbrayer, M. Murray, C. Rogan, S. Sanders, E. Schmitz, J.D. Tapia Takaki, Q. Wang

Kansas State University, Manhattan, USA
S. Duric, A. Ivanov, K. Kaadze, D. Kim, Y. Maravin, D.R. Mendis, T. Mitchell, A. Modak, A. Mohammadi, L.K. Saini

Lawrence Livermore National Laboratory, Livermore, USA
F. Rebassoo, D. Wright

University of Maryland, College Park, USA
A. Baden, O. Baron, A. Belloni, S.C. Eno, Y. Feng, C. Ferraioli, N.J. Hadley, S. Jabeen, G.Y. Jeng, R.G. Kellogg, J. Kunkle, A.C. Mignerey, S. Nabili, F. Ricci-Tam, Y.H. Shin, A. Skuja, S.C. Tonwar, K. Wong

Massachusetts Institute of Technology, Cambridge, USA
D. Abercrombie, B. Allen, V. Azzolini, A. Baty, G. Bauer, R. Bi, S. Brandt, W. Busza, I.A. Cali, M. D'Alfonso, Z. Demiragli, G. Gomez Ceballos, M. Goncharov, P. Harris, D. Hsu, M. Hu, Y. Iiyama, G.M. Innocenti, M. Klute, D. Kovalskyi, Y.-J. Lee, P.D. Luckey, B. Maier, A.C. Marini, C. Mcginn, C. Mironov, S. Narayanan, X. Niu, C. Paus, C. Roland, G. Roland, Z. Shi, G.S.F. Stephans, K. Sumorok, K. Tatar, D. Velicanu, J. Wang, T.W. Wang, B. Wyslouch

University of Minnesota, Minneapolis, USA
A.C. Benvenuti[†], R.M. Chatterjee, A. Evans, P. Hansen, J. Hiltbrand, Sh. Jain, S. Kalafut, M. Krohn, Y. Kubota, Z. Lesko, J. Mans, N. Ruckstuhl, R. Rusack, M.A. Wadud

University of Mississippi, Oxford, USA
J.G. Acosta, S. Oliveros

University of Nebraska-Lincoln, Lincoln, USA
E. Avdeeva, K. Bloom, D.R. Claes, C. Fangmeier, F. Golf, R. Gonzalez Suarez, R. Kamalieddin, I. Kravchenko, J. Monroy, J.E. Siado, G.R. Snow, B. Stieger

State University of New York at Buffalo, Buffalo, USA
A. Godshalk, C. Harrington, I. Iashvili, A. Kharchilava, C. Mclean, D. Nguyen, A. Parker, S. Rappoccio, B. Roozbahani

Northeastern University, Boston, USA
G. Alverson, E. Barberis, C. Freer, Y. Haddad, A. Hortiangtham, D.M. Morse, T. Orimoto, R. Teixeira De Lima, T. Wamorkar, B. Wang, A. Wisecarver, D. Wood

Northwestern University, Evanston, USA
S. Bhattacharya, J. Bueghly, O. Charaf, K.A. Hahn, N. Mucia, N. Odell, M.H. Schmitt, K. Sung, M. Trovato, M. Velasco

University of Notre Dame, Notre Dame, USA
R. Bucci, N. Dev, M. Hildreth, K. Hurtado Anampa, C. Jessop, D.J. Karmgard, N. Kellams, K. Lannon, W. Li, N. Loukas, N. Marinelli, F. Meng, C. Mueller, Y. Musienko[35], M. Planer, A. Reinsvold, R. Ruchti, P. Siddireddy, G. Smith, S. Taroni, M. Wayne, A. Wightman, M. Wolf, A. Woodard

The Ohio State University, Columbus, USA
J. Alimena, L. Antonelli, B. Bylsma, L.S. Durkin, S. Flowers, B. Francis, C. Hill, W. Ji, T.Y. Ling, W. Luo, B.L. Winer

Princeton University, Princeton, USA
S. Cooperstein, P. Elmer, J. Hardenbrook, S. Higginbotham, A. Kalogeropoulos, D. Lange, M.T. Lucchini, J. Luo, D. Marlow, K. Mei, I. Ojalvo, J. Olsen, C. Palmer, P. Piroué, J. Salfeld-Nebgen, D. Stickland, C. Tully, Z. Wang

University of Puerto Rico, Mayaguez, USA
S. Malik, S. Norberg

Purdue University, West Lafayette, USA
A. Barker, V.E. Barnes, S. Das, L. Gutay, M. Jones, A.W. Jung, A. Khatiwada, B. Mahakud, D.H. Miller, N. Neumeister, C.C. Peng, S. Piperov, H. Qiu, J.F. Schulte, J. Sun, F. Wang, R. Xiao, W. Xie

Purdue University Northwest, Hammond, USA
T. Cheng, J. Dolen, N. Parashar

Rice University, Houston, USA
Z. Chen, K.M. Ecklund, S. Freed, F.J.M. Geurts, M. Kilpatrick, W. Li, B.P. Padley, R. Redjimi, J. Roberts, J. Rorie, W. Shi, Z. Tu, A. Zhang

University of Rochester, Rochester, USA
A. Bodek, P. de Barbaro, R. Demina, Y.t. Duh, J.L. Dulemba, C. Fallon, T. Ferbel, M. Galanti, A. Garcia-Bellido, J. Han, O. Hindrichs, A. Khukhunaishvili, E. Ranken, P. Tan, R. Taus

Rutgers, The State University of New Jersey, Piscataway, USA
A. Agapitos, J.P. Chou, Y. Gershtein, E. Halkiadakis, A. Hart, M. Heindl, E. Hughes, S. Kaplan, R. Kunnawalkam Elayavalli, S. Kyriacou, A. Lath, R. Montalvo, K. Nash, M. Osherson, H. Saka, S. Salur, S. Schnetzer, D. Sheffield, S. Somalwar, R. Stone, S. Thomas, P. Thomassen, M. Walker

University of Tennessee, Knoxville, USA
A.G. Delannoy, J. Heideman, G. Riley, S. Spanier

Texas A&M University, College Station, USA
O. Bouhali[72], A. Celik, M. Dalchenko, M. De Mattia, A. Delgado, S. Dildick, R. Eusebi, J. Gilmore, T. Huang, T. Kamon[73], S. Luo, R. Mueller, D. Overton, L. Perniè, D. Rathjens, A. Safonov

Texas Tech University, Lubbock, USA
N. Akchurin, J. Damgov, F. De Guio, P.R. Dudero, S. Kunori, K. Lamichhane, S.W. Lee, T. Mengke, S. Muthumuni, T. Peltola, S. Undleeb, I. Volobouev, Z. Wang

Vanderbilt University, Nashville, USA
S. Greene, A. Gurrola, R. Janjam, W. Johns, C. Maguire, A. Melo, H. Ni, K. Padeken, J.D. Ruiz Alvarez, P. Sheldon, S. Tuo, J. Velkovska, M. Verweij, Q. Xu

University of Virginia, Charlottesville, USA
M.W. Arenton, P. Barria, B. Cox, R. Hirosky, M. Joyce, A. Ledovskoy, H. Li, C. Neu, T. Sinthuprasith, Y. Wang, E. Wolfe, F. Xia

Wayne State University, Detroit, USA
R. Harr, P.E. Karchin, N. Poudyal, J. Sturdy, P. Thapa, S. Zaleski

University of Wisconsin - Madison, Madison, WI, USA
M. Brodski, J. Buchanan, C. Caillol, D. Carlsmith, S. Dasu, I. De Bruyn, L. Dodd, B. Gomber, M. Grothe, M. Herndon, A. Hervé, U. Hussain, P. Klabbers, A. Lanaro, K. Long, R. Loveless, T. Ruggles, A. Savin, V. Sharma, N. Smith, W.H. Smith, N. Woods

†: Deceased
1: Also at Vienna University of Technology, Vienna, Austria
2: Also at IRFU, CEA, Université Paris-Saclay, Gif-sur-Yvette, France
3: Also at Universidade Estadual de Campinas, Campinas, Brazil
4: Also at Federal University of Rio Grande do Sul, Porto Alegre, Brazil
5: Also at Université Libre de Bruxelles, Bruxelles, Belgium
6: Also at University of Chinese Academy of Sciences, Beijing, China
7: Also at Institute for Theoretical and Experimental Physics, Moscow, Russia
8: Also at Joint Institute for Nuclear Research, Dubna, Russia
9: Also at Cairo University, Cairo, Egypt
10: Also at Helwan University, Cairo, Egypt
11: Now at Zewail City of Science and Technology, Zewail, Egypt
12: Also at Department of Physics, King Abdulaziz University, Jeddah, Saudi Arabia
13: Also at Université de Haute Alsace, Mulhouse, France
14: Also at Skobeltsyn Institute of Nuclear Physics, Lomonosov Moscow State University, Moscow, Russia
15: Also at CERN, European Organization for Nuclear Research, Geneva, Switzerland
16: Also at RWTH Aachen University, III. Physikalisches Institut A, Aachen, Germany
17: Also at University of Hamburg, Hamburg, Germany
18: Also at Brandenburg University of Technology, Cottbus, Germany
19: Also at Institute of Physics, University of Debrecen, Debrecen, Hungary
20: Also at Institute of Nuclear Research ATOMKI, Debrecen, Hungary
21: Also at MTA-ELTE Lendület CMS Particle and Nuclear Physics Group, Eötvös Loránd University, Budapest, Hungary
22: Also at Indian Institute of Technology Bhubaneswar, Bhubaneswar, India

23: Also at Institute of Physics, Bhubaneswar, India
24: Also at Shoolini University, Solan, India
25: Also at University of Visva-Bharati, Santiniketan, India
26: Also at Isfahan University of Technology, Isfahan, Iran
27: Also at Plasma Physics Research Center, Science and Research Branch, Islamic Azad University, Tehran, Iran
28: Also at Università degli Studi di Siena, Siena, Italy
29: Also at Scuola Normale e Sezione dell'INFN, Pisa, Italy
30: Also at Kyunghee University, Seoul, Korea
31: Also at International Islamic University of Malaysia, Kuala Lumpur, Malaysia
32: Also at Malaysian Nuclear Agency, MOSTI, Kajang, Malaysia
33: Also at Consejo Nacional de Ciencia y Tecnología, Mexico City, Mexico
34: Also at Warsaw University of Technology, Institute of Electronic Systems, Warsaw, Poland
35: Also at Institute for Nuclear Research, Moscow, Russia
36: Now at National Research Nuclear University 'Moscow Engineering Physics Institute' (MEPhI), Moscow, Russia
37: Also at St. Petersburg State Polytechnical University, St. Petersburg, Russia
38: Also at University of Florida, Gainesville, USA
39: Also at P.N. Lebedev Physical Institute, Moscow, Russia
40: Also at California Institute of Technology, Pasadena, USA
41: Also at Budker Institute of Nuclear Physics, Novosibirsk, Russia
42: Also at Faculty of Physics, University of Belgrade, Belgrade, Serbia
43: Also at INFN Sezione di Pavia [a], Università di Pavia [b], Pavia, Italy
44: Also at University of Belgrade, Faculty of Physics and Vinca Institute of Nuclear Sciences, Belgrade, Serbia
45: Also at National and Kapodistrian University of Athens, Athens, Greece
46: Also at Riga Technical University, Riga, Latvia
47: Also at Universität Zürich, Zurich, Switzerland
48: Also at Stefan Meyer Institute for Subatomic Physics (SMI), Vienna, Austria
49: Also at Istanbul Aydin University, Istanbul, Turkey
50: Also at Mersin University, Mersin, Turkey
51: Also at Piri Reis University, Istanbul, Turkey
52: Also at Gaziosmanpasa University, Tokat, Turkey
53: Also at Adiyaman University, Adiyaman, Turkey
54: Also at Ozyegin University, Istanbul, Turkey
55: Also at Izmir Institute of Technology, Izmir, Turkey
56: Also at Marmara University, Istanbul, Turkey
57: Also at Kafkas University, Kars, Turkey
58: Also at Istanbul University, Faculty of Science, Istanbul, Turkey
59: Also at Istanbul Bilgi University, Istanbul, Turkey
60: Also at Hacettepe University, Ankara, Turkey
61: Also at Rutherford Appleton Laboratory, Didcot, United Kingdom
62: Also at School of Physics and Astronomy, University of Southampton, Southampton, United Kingdom
63: Also at Monash University, Faculty of Science, Clayton, Australia
64: Also at Bethel University, St. Paul, USA
65: Also at Karamanoğlu Mehmetbey University, Karaman, Turkey
66: Also at Utah Valley University, Orem, USA
67: Also at Purdue University, West Lafayette, USA

68: Also at Beykent University, Istanbul, Turkey
69: Also at Bingol University, Bingol, Turkey
70: Also at Sinop University, Sinop, Turkey
71: Also at Mimar Sinan University, Istanbul, Istanbul, Turkey
72: Also at Texas A&M University at Qatar, Doha, Qatar
73: Also at Kyungpook National University, Daegu, Korea